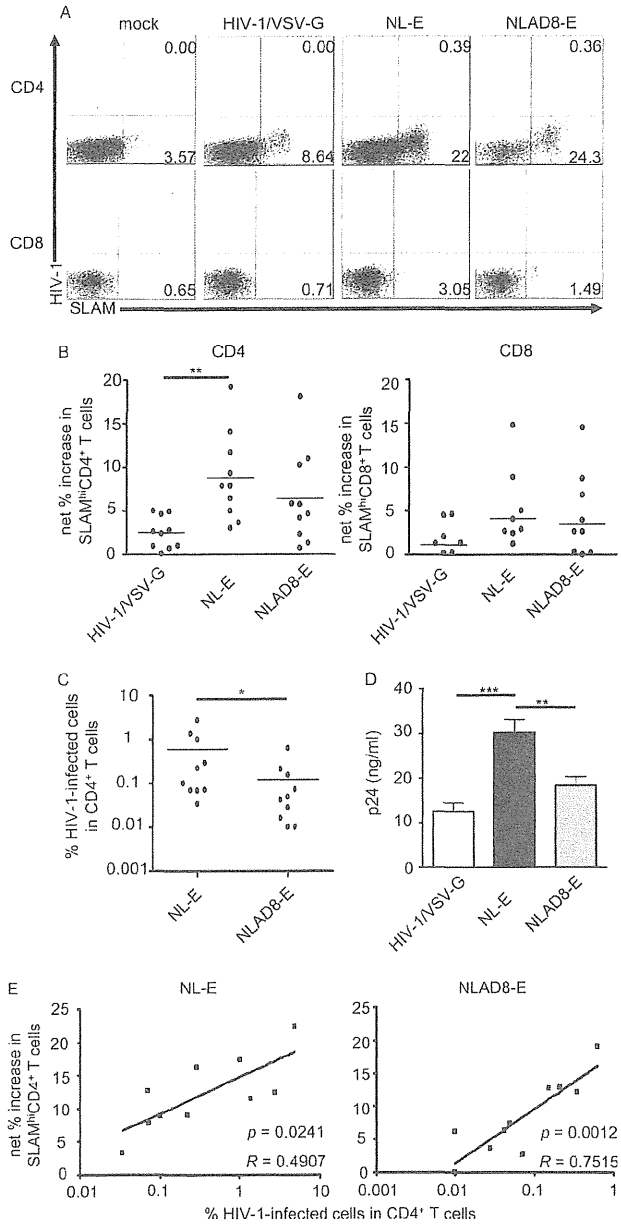


FIG 2 SLAM expression on $CD4^+$ T cells within the HIV-1-infected PBMC population. (A and B) PBMCs were infected with HIV-1/VSV-G, HIV-$1_{NL-E}$, or HIV-$1_{NLAD8-E}$, and SLAM expression on $CD4^+$ T cells was analyzed. (A) Representative flow cytometry plots showing SLAM expression on $CD4^+$ T cells and $CD8^+$ T cells. (B) Cumulative data showing the percent increase in the frequency of $SLAM^{hi}$ $CD4^+$ and $SLAM^{hi}$ $CD8^+$ T cells from 10 donors. *P* values were calculated using one-way analysis of variance followed by the Tukey multiple-comparison test. **, $P < 0.01$. (C) Cumulative data showing the frequency of HIV-1-infected $CD4^+$ T cells from 10 donors. *P* values were calculated using the Mann-Whitney U test. *, $P < 0.05$. (D) Levels of p24 antigen in culture supernatants of HIV-1-infected PBMCs. The bars represent the mean ± SEM ($n = 10$). *P* values were calculated using one-way analysis of variance followed by the Tukey multiple-comparison test. **, $P < 0.01$; ***, $P < 0.001$. (E) Correlation between the frequency of HIV-$1_{NL-E}$- and HIV-$1_{NLAD8-E}$-infected $CD4^+$ T cells and the percent increase in the frequency of $SLAM^{hi}$ $CD4^+$ T cells from 10 donors. Correlation statistics were analyzed using the Pearson correlation.

($GFP^+$) cells were scarcely detectable under these conditions, probably reflecting the low transduction efficiency of VSV-pseudotyped lentivirus in unstimulated T cells. A marked upregulation of SLAM expression induced by HIV-$1_{NLAD8-E}$ infection was also observed in some donors, but the difference between HIV-$1_{NLAD8-E}$- and HIV-1/VSV-G-infected cultures was not statistically significant (Fig. 2B). This probably reflects the variable number and low frequency of $CCR5^+$ $CD4^+$ T cells (5 to 10% of $CD4^+$ T cells), which are a target of CCR5-tropic HIV-$1_{NLAD8-E}$, in donor PBMCs. As expected, the frequency of HIV-$1_{NL-E}$-infected $CD4^+$ T cells (0.88% ± 0.28%) was higher than that of HIV-$1_{NLAD8-E}$-infected $CD4^+$ T cells (0.19% ± 0.01%) ($P = 0.0433$; $n = 10$; Fig. 2C). In parallel with the high frequency of $SLAM^{hi}$ $CD4^+$ T cells, the levels of p24 were the highest in the culture supernatants of HIV-$1_{NL-E}$-infected cultures compared to other HIV-1-infected cultures (Fig. 2D). There was a significant correlation between the frequency of HIV-1-infected $CD4^+$ T cells and that of $SLAM^{hi}$ $CD4^+$ T cells in both HIV-$1_{NL-E}$-infected ($R = 0.4907$, $P = 0.0241$; $n = 10$) and HIV-$1_{NLAD8-E}$-infected ($R = 0.7517$; $P = 0.0012$; $n = 10$) cultures (Fig. 2E).

To determine whether the replication of HIV-1 was required for SLAM upregulation, PBMCs were infected with a 20-fold higher dose of HIV-1/VSV-G. The frequency of $GFP^+$ $CD4^+$ T cells and $SLAM^{hi}$ $CD4^+$ T cells under these conditions was identical to that seen in HIV-$1_{NL-E}$-infected PBMCs (see Fig. S1 in the supplemental material). Taken together, these results indicated that HIV-1 replication is not essential but that higher and/or persistent levels of HIV-1 are involved in the upregulation of SLAM expression on $CD4^+$ T cells.

All subsequent studies were carried out using CXCR4-tropic HIV-$1_{NL-E}$.

**SLAM upregulation by HIV-1 infection is not caused by direct infection of $CD4^+$ T cells.** Despite the fact that HIV-1 infection enhanced SLAM expression on $CD4^+$ T cells, upregulation was more obvious in HIV-1-uninfected $CD4^+$ T cells (Fig. 2A). To further test the importance of direct HIV-1 infection of $CD4^+$ T cells for SLAM upregulation, T cells were enriched from PBMCs. PBMCs and T cells were separately infected with HIV-$1_{NL-E}$, and the expression of SLAM on $CD4^+$ T cells was analyzed after 5 days of culture. A representative result from six individuals is shown in Fig. 3A, and plots from all six individuals are shown, with averages, in Fig. 3B. The majority of HIV-$1_{NL-E}$-infected $CD4^+$ T cells in the purified T cell cultures were SLAM-dull (Fig. 3A), and the net increase in the frequency of $SLAM^{hi}$ $CD4^+$ T cells (2.87% ± 1.04%) was much lower than that in the PBMC cultures (13.00% ± 3.72%) ($P < 0.01$; $n = 6$; Fig. 3B). To examine in more detail which cell population within the PBMCs contributed to the upregulation of SLAM by HIV-1 infection, whole PBMCs and those depleted of either $CD14^+$ monocytes, $CD19^+$ B cells, or $HLA\text{-}DR^+$ cells were infected with HIV-$1_{NL-E}$. Cell depletion was evaluated by flow cytometry (Fig. 3C). The removal of $HLA\text{-}DR^+$ cells resulted in depletion of both monocytes and B cells (Fig. 3C, lower right). Of note, a minor population of CD123-, CD141-, and/or CD303-expressing cells (peripheral dendritic cells [pDCs] and conventional dendritic cells [DCs]) were also removed by depletion of $HLA\text{-}DR^+$ cells (data not shown). There were no significant differences in the increase in $SLAM^{hi}$ $CD4^+$ T cells among monocyte- and B cell-depleted PBMCs compared to whole PBMCs following HIV-1 infection in four donors; the relative increases in monocyte- and B cell-depleted PBMCs compared to

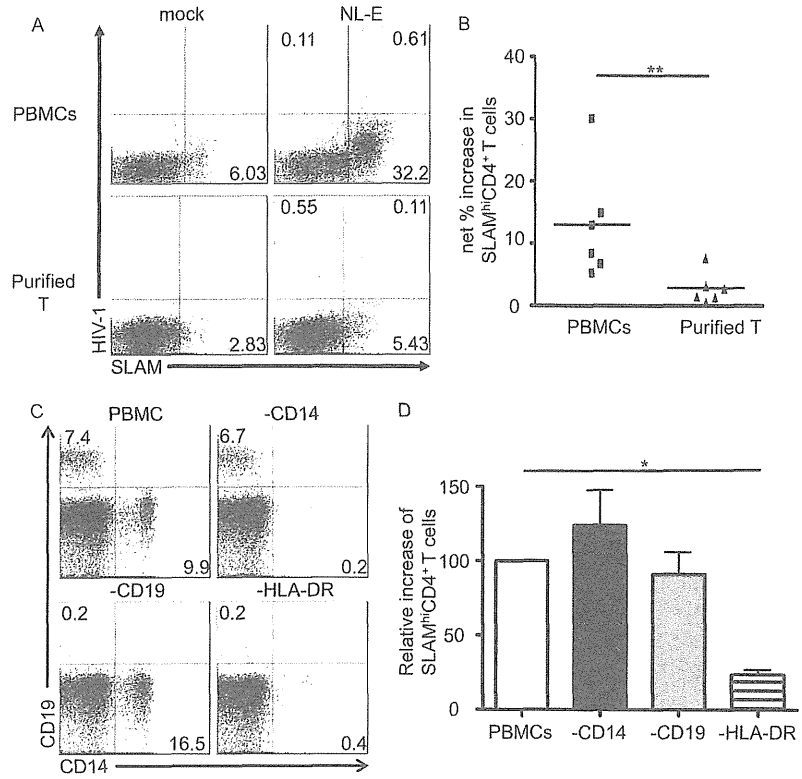


FIG 3 Comparison of the levels of SLAM upregulation on $CD4^+$ T cells induced by HIV-1 infection in the presence or absence of non-T cells. (A and B) Purified T cells and PBMCs were separately infected with HIV-$1_{NL-E}$. (A) Representative flow cytometry plots showing SLAM expression on $CD4^+$ T cells. (B) Cumulative data showing the percent increase in $SLAM^{hi}$ $CD4^+$ T cells. The bars represent the mean ± SEM ($n = 6$). $P$ values were calculated using the Mann-Whitney U test. **, $P < 0.01$. (C and D) PBMCs were infected with HIV-$1_{NL-E}$ after removal of monocytes, B cells, or HLA-$DR^+$ cells. (C) Representative flow cytometry plot evaluating the depletion of monocytes, B cells, or HLA-$DR^+$ cells. (D) Cumulative data showing the relative increase in the frequency of $SLAM^{hi}$ $CD4^+$ T cells. The increase in the frequency of $SLAM^{hi}$ $CD4^+$ T cells by HIV-1 infection in the PBMC population was set to 100%. The bars represent the mean ± SEM ($n = 4$). $P$ values were calculated using one-way analysis of variance followed by the Tukey multiple-comparison test. *, $P < 0.05$.

whole PBMCs (set at 100%) were 124.1% ± 23.68% and 91.19% ± 14.84%, respectively ($n = 4$). In contrast, SLAM expression was significantly repressed in HLA-$DR^+$ cell-depleted PBMCs following HIV-1 infection (relative increase, 23.65% ± 3.13%; $n = 4$). Taken together, these results indicated that a population of HLA-DR-expressing cells, including DCs, but not monocytes and B cells, is involved in the upregulation of SLAM by HIV-1 infection.

**Role of cytokines in induction of SLAM expression during HIV infection.** SLAM expression on T cells and DCs is upregulated by IFN-γ (9) and IL-1β (14), respectively. Therefore, the levels of 11 cytokines (IFN-γ, IL-1β, IL-2, IL-4, IL-5, IL-6, IL-8, IL-10, IL-12 p70, TNF-α, and TNF-β) in the culture supernatants of HIV-$1_{NL-E}$-infected and -uninfected PBMCs were measured at day 5. The results showed that the production of IFN-γ, IL-1β, and TNF-α in HIV-$1_{NL-E}$-infected PBMCs was significantly higher than that in uninfected PBMCs ($P = 0.0006$, 0.0023, and 0.0041, respectively; $n = 4$; Fig. 4A). The levels of IL-2, IL-4, IL-5, IL-6, IL-8, IL-10, IL-12 p70, and TNF-β were low or undetectable, irrespective of HIV-1 infection (data not shown). SLAM upregulation on $CD4^+$ T cells was not affected, when HIV-$1_{NL-E}$-infected PBMCs were cultured in the absence or presence of anti-IFN-γ blocking MAb (data not shown). Furthermore, SLAM upregulation was not observed in PBMC cultures in the presence of recombinant IFN-γ (data not shown).

To test the potential contribution of any soluble factors produced in HIV-1-infected PBMC cultures, we performed a transwell assay. HIV-$1_{NL-E}$-infected PBMCs were seeded into the top chamber of the transwell, and uninfected PBMCs were placed in the bottom chamber. The cells were then cultured for 5 days. A representative result is shown in Fig. 4B. SLAM was markedly upregulated in HIV-$1_{NL-E}$-infected PBMCs in the top chamber (net increase, 32.81%; Fig. 4B, upper right), whereas upregulation was less obvious in uninfected PBMCs in the bottom chamber (net increase, 3.35%; Fig. 4B, lower right). The result was reproduced using PBMCs from eight separate donors, and the difference was statistically significant (bottom chamber, 1.07% ± 0.80%; top chamber, 9.08% ± 4.60%; $P < 0.001$; $n = 5$; Fig. 4C). Thus, these data clearly show that soluble factors produced by HIV-1 infection make a minimal contribution (if any) to SLAM upregulation on $CD4^+$ T cells. Rather, cell-to-cell contact would appear to be the most important factor.

**Importance of costimulatory molecules for SLAM upregulation on $CD4^+$ T cells.** SLAM expression on T cells is induced by T cell receptor (TcR) stimulation with anti-CD3 antibody (3). In addition, Sheng and colleagues showed that LFA-3/CD2 interaction and, particularly, CD2 signaling are necessary but not sufficient for $CD4^+$ T cell activation (25). We showed earlier that in PBMCs, HLA-$DR^+$ cells are largely responsible for the upregulation of SLAM after HIV-1 infection (Fig. 3C). Previously, we

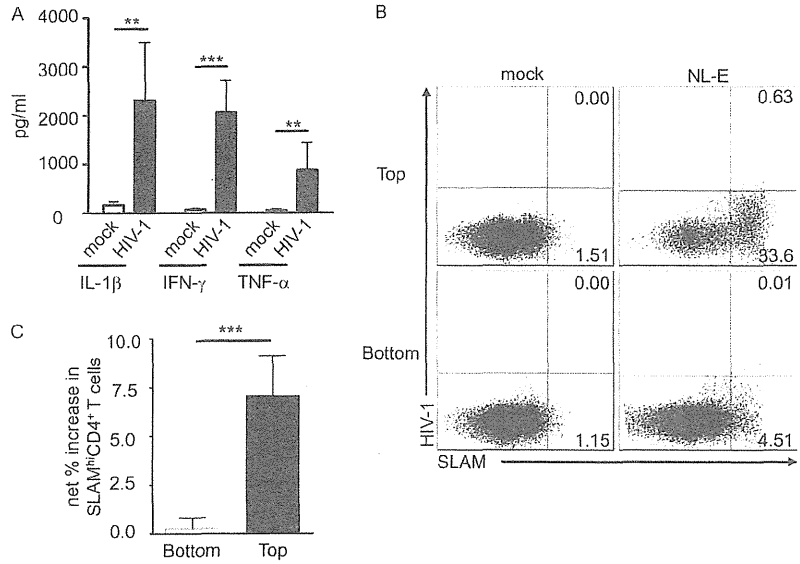


FIG 4 Impact of soluble factors on SLAM upregulation by HIV-1-infected $CD4^+$ T cells. (A) PBMCs were infected with $HIV\text{-}1_{NL\text{-}E}$, and the cytokine levels in the culture supernatants were measured. The bars represent the mean ± SEM ($n = 7$). $P$ values were calculated using the Mann-Whitney U test. **, $P < 0.01$; ***, $P < 0.001$. (B and C) $HIV\text{-}1_{NL\text{-}E}$- and mock-infected PBMCs were cultured in the top chamber and uninfected PBMCs were placed in the bottom chamber of a transwell plate. (B) Representative flow cytometry plots showing SLAM expression on $CD4^+$ T cells. (C) Percent increase in the frequency of $SLAM^{hi}$ $CD4^+$ T cells. The bars represent the mean ± SEM ($n = 8$). $P$ values were calculated using the Mann-Whitney U test. ***, $P < 0.001$.

showed that HIV-1 replication and expansion are associated with the activation of $CD4^+$ T cells through cell-to-cell contact with monocyte-derived DCs via costimulatory molecules such as LFA-1/intercellular adhesion molecule 1 (ICAM-1) and LFA-3/CD2 (27). We next tested the effect of blocking antibodies that inhibited these interactions on SLAM expression on $CD4^+$ T cells. $HIV\text{-}1_{NL\text{-}E}$-infected PBMCs were cultured in the absence or presence of blocking MAbs against LFA-1α and LFA-3. As shown in Fig. 5A, increased SLAM expression on $CD4^+$ T cells within the $HIV\text{-}1_{NL\text{-}E}$-infected PBMC population was inhibited by anti-LFA-1α MAb (48.81% ± 18.12%; $n = 5$) as well as by anti-LFA-3 MAb (86.58% ± 6.93%; $n = 5$), although the effect of anti-LFA-1α MAb was less pronounced and was not statistically significant at 10 μg/ml (Fig. 5B). Nevertheless, both anti-LFA-1α and anti-LFA-3 MAbs inhibited SLAM upregulation in a dose-dependent manner (Fig. 5C), and the in-

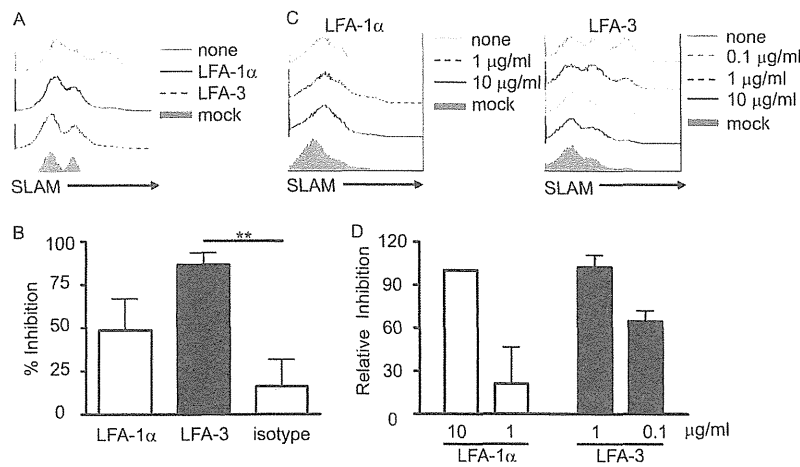


FIG 5 Role of cell-to-cell contact in SLAM upregulation on HIV-1-infected $CD4^+$ T cells. (A and B) $HIV\text{-}1_{NL\text{-}E}$-infected PBMCs were cultured in the presence of 10 μg/ml of anti-LFA-1α or anti-LFA-3 MAbs or isotype control IgG1. (A) Representative histogram showing SLAM expression on $CD4^+$ T cells. (B) Percent inhibition of the increase in the frequency of $SLAM^{hi}$ $CD4^+$ T cells. The frequency of $SLAM^{hi}$ $CD4^+$ T cells upregulated by HIV-1 infection was arbitrarily designated 100%. The bars represent the mean ± SEM ($n = 5$). $P$ values were calculated using one-way analysis of variance followed by the Tukey multiple-comparison test. **, $P < 0.01$. (C and D) $HIV\text{-}1_{NL\text{-}E}$-infected PBMCs were cultured in the presence of serially diluted concentrations of anti-LFA-1α or anti-LFA-3 MAbs. (C) Representative histogram showing SLAM expression on $CD4^+$ T cells cultured with anti-LFA-1α (left) or anti-LFA-3 (right) MAbs. (D) Relative inhibition of the increase in the frequency of $SLAM^{hi}$ $CD4^+$ T cells. The percent inhibition in the frequency of $SLAM^{hi}$ $CD4^+$ T cells by 10 μg/ml of anti-LFA-1α or anti-LFA-3 MAbs was arbitrarily designated 100%. The bars represent the mean ± SEM ($n = 3$).

hibitory effect of anti-LFA-3 MAb was observed at concentrations as low as 0.1 μg/ml (Fig. 5D).

To confirm whether the inhibition of HIV-1-associated SLAM upregulation by these blocking antibodies also resulted in reduced MV infectivity in $CD4^+$ T cells, HIV-$1_{NL-D}$-infected PBMCs cultured in the presence of blocking antibodies were infected with MVwt ($n = 2$). As expected, although the frequency of MVwt-infected $CD4^+$ T cells was increased by HIV-1 infection (from 1.30% to 4.51% for donor 1 and from 2.59% to 7.63% for donor 2), the frequency of MVwt-infected cells was reduced by anti-LFA-1α (1.21% and 5.01% for donor 1 and donor 2, respectively) and more strongly by anti-LFA-3 (1.34% and 3.63% for donor 1 and donor 2, respectively) (see Fig. S2 in the supplemental material). These data clearly indicate that SLAM upregulation and the resulting increase in MV-infected $CD4^+$ T cells are mediated by cell-to-cell contact through the interaction of costimulatory molecules that are highly expressed on HLA-$DR^+$ DC subsets in HIV-1-infected PBMC cultures.

## DISCUSSION

The present study shows that HIV-1 infection enhanced MV infection in $CD4^+$ T cells. Interestingly, we observed that the frequencies of MVvac-infected $CD4^+$ T cells were higher than those of MVwt in both HIV-1-infected and -uninfected PBMCs. This difference may be explained by different receptor usage (4) and by differences in polymerase activity between the wild-type and vaccine strains (1) used in this study. In addition, both strains of MV inhibited HIV-1 replication (Fig. 1C), which is consistent with previous reports (7, 8, 10). Although the precise mechanism(s) underlying HIV-1 suppression by MV is not completely understood, the reduction of p24 antigen observed in the culture supernatant occurred in parallel with the elimination of HIV-1-infected cells after MV infection. It is speculated that MV infection causes apoptosis of HIV-1-infected cells directly through the expression of viral nucleoprotein and hemagglutinin proteins (2, 13, 15, 28) or through the induction of cell $G_0/G_1$ arrest (8), although no doubly infected $CD4^+$ T cells were detected in the culture system used in the present study. Alternatively, considering the fact that HIV-1-infected $CD4^+$ T cells are already activated, they may be hyperactivated by MV, resulting in activation-induced cell death (11).

Because MV utilizes SLAM as a receptor, it is very likely that the enhanced MV infection observed in this *ex vivo* MV and HIV-1 coinfection model was due to HIV-1-induced upregulation of SLAM. Meroni et al. showed that SLAM expression on $CD4^+$ T cells *ex vivo* is diminished during the early phase of HIV infection (16). In addition, SLAM expression on $CD4^+$ T cells was different in patients recently and chronically infected with HIV-1 (16). SLAM expression on $CD4^+$ T cells from HIV-1-infected individuals may fluctuate depending on the activation state of the immune system *in vivo*. It is important to note that most $CD4^+$ T cells within the *ex vivo* PBMC population were in the resting state and that SLAM expression was transiently downregulated soon after the initiation of culture (unpublished observation). SLAM is expressed on activated cells, and chronic hyperactivation is a characteristic feature of HIV-1 infection (11). It was assumed that $CD4^+$ T cells in the PBMC cultures were not hyperactivated and were, rather, akin to the cells within the lymphoid organs, in which a variety of antigen-presenting cells (APCs) and T cells are in contact with each other and where HIV-1 replication/expansion occurs. Therefore, it is possible that SLAM expression is upregulated in lymphoid organs during HIV-1 infection, which may enhance the infectivity of MV.

One of the aims of the present study was to examine the mechanism(s) by which HIV-1 infection enhances SLAM expression on $CD4^+$ T cells. IFN-γ upregulates SLAM expression on T cells in patients with tuberculosis (9, 23). However, neither IFN-γ nor any other soluble factors played a major role in the SLAM upregulation observed in this study. It is possible that SLAM upregulation by IFN-γ is a specific feature of certain T cells reactive to *Mycobacterium tuberculosis*. Nevertheless, the low level of SLAM upregulation induced in T cell culture may be mediated by cytokines, including IFN-γ.

In the present study, blocking experiments showed that cell-to-cell contact (presumably DCs to $CD4^+$ T cells) via LFA-1/ICAM-1 and LFA-3/CD2 interactions enhanced SLAM expression on $CD4^+$ T cells (Fig. 5). Inhibition of the LFA-3/CD2 interaction led to a more marked abrogation of SLAM expression than inhibition of the LFA-1/ICAM-1 interaction. It is noteworthy that a previous study also showed that the LFA-3/CD2 interaction was more important than the LFA-1/ICAM-1 interaction for antigen-dependent DC-T cell synapse formation (27). Therefore, CD2 costimulatory signals, in addition to TcR signals, may be involved in SLAM upregulation. Potential candidate APCs that interact with $CD4^+$ T cells to upregulate SLAM on $CD4^+$ T cells in HIV-infected PBMC cultures could be HLA-$DR^+$ DCs.

In conclusion, the precise mechanism(s) by which MV exacerbates the disease outcomes in HIV-1-infected individuals remains unknown. The present study, which employed a PBMC-based *ex vivo* HIV-1 and MV coinfection model, showed that increased susceptibility to MV infection involves induction of a high level of SLAM expression by HIV-1 infection via cell-to-cell contact. This is the first report showing a direct relationship between HIV-1 infection and SLAM expression. The high mortality and morbidity of measles in children coinfected with HIV-1 and MV may be due to upregulation of SLAM expression on $CD4^+$ T cells, which presumably occurs within lymphoid organs through T cell contact with DCs during HIV-1 infection. Further *in vivo* coinfection studies in a macaque model should help to clarify these outstanding issues.

## ACKNOWLEDGMENTS

We thank Kahori Okano for her excellent technical assistance.

This work was supported by a grant from the Ministry of Health, Labor, and Welfare of Japan. Y.-Y. Mitsuki receives support from the Japanese Foundation for AIDS Prevention.

## REFERENCES

1. **Bankamp B, Kearney SP, Liu X, Bellini WJ, Rota PA.** 2002. Activity of polymerase proteins of vaccine and wild-type measles virus strains in a minigenome replication assay. J. Virol. 76:7073–7081.
2. **Bhaskar A, Bala J, Varshney A, Yadava P.** 2011 Expression of measles virus nucleoprotein induces apoptosis and modulates diverse functional proteins in cultured mammalian cells. PLoS One 6:e18765. doi:10.1371/journal.pone.0018765.
3. **Cocks BG, et al.** 1995. A novel receptor involved in T-cell activation. Nature 376:260–263.
4. **Condack C, Grivel JC, Devaux P, Margolis L, Cattaneo R.** 2007. Measles virus vaccine attenuation: suboptimal infection of lymphatic tissue and tropism alteration. J. Infect. Dis. 196:541–549.
5. **Erlenhoefer C, et al.** 2001. CD150 (SLAM) is a receptor for measles virus but is not involved in viral contact-mediated proliferation inhibition. J. Virol. 75:4499–4505.

6. **Fujino M, et al.** 2007. Development of a new neutralization test for measles virus. J. Virol. Methods 142:15–20.
7. **Garcia M, Yu XF, Griffin DE, Moss WJ.** 2005. In vitro suppression of human immunodeficiency virus type 1 replication by measles virus. J. Virol. 79:9197–9205.
8. **Garcia M, Yu XF, Griffin DE, Moss WJ.** 2008. Measles virus inhibits human immunodeficiency virus type 1 reverse transcription and replication by blocking cell-cycle progression of CD4+ T lymphocytes. J. Gen. Virol. 89:984–993.
9. **Garcia VE, et al.** 2001. Signaling lymphocytic activation molecule expression and regulation in human intracellular infection correlate with Th1 cytokine patterns. J. Immunol. 167:5719–5724.
10. **Grivel JC, Garcia M, Moss WJ, Margolis LB.** 2005. Inhibition of HIV-1 replication in human lymphoid tissues ex vivo by measles virus. J. Infect. Dis. 192:71–78.
11. **Haas A, Zimmermann K, Oxenius A.** 2011. Antigen-dependent and -independent mechanisms of T and B cell hyperactivation during chronic HIV-1 infection. J. Virol. 85:12102–12113.
12. **Hashimoto K, et al.** 2002. SLAM (CD150)-independent measles virus entry as revealed by recombinant virus expressing green fluorescent protein. J. Virol. 76:6743–6749.
13. **Iwasa T, Suga S, Qi L, Komada Y.** 2010. Apoptosis of human peripheral blood mononuclear cells by wild-type measles virus infection is induced by interaction of hemagglutinin protein and cellular receptor, SLAM via caspase-dependent pathway. Microbiol. Immunol. 54:405–416.
14. **Kruse M, et al.** 2001. Signaling lymphocytic activation molecule is expressed on mature CD83+ dendritic cells and is up-regulated by IL-1 beta. J. Immunol. 167:1989–1995.
15. **Laine D, et al.** 2005. Measles virus nucleoprotein induces cell-proliferation arrest and apoptosis through NTAIL-NR and NCORE-FcgammaRIIB1 interactions, respectively. J. Gen. Virol. 86:1771–1784.
16. **Meroni L, et al.** 1999. Altered signaling lymphocytic activation molecule (SLAM) expression in HIV infection and redirection of HIV-specific responses via SLAM triggering. Clin. Immunol. 92:276–284.
17. **Moss WJ, Cutts F, Griffin DE.** 1999. Implications of the human immunodeficiency virus epidemic for control and eradication of measles. Clin. Infect. Dis. 29:106–112.
18. **Moss WJ, et al.** 2008. HIV type 1 infection is a risk factor for mortality in hospitalized Zambian children with measles. Clin. Infect. Dis. 46: 523–527.
19. **Moss WJ, et al.** 2007. Immunogenicity of standard-titer measles vaccine in HIV-1-infected and uninfected Zambian children: an observational study. J. Infect. Dis. 196:347–355.
20. **Muhlebach MD, et al.** 2011. Adherens junction protein nectin-4 is the epithelial receptor for measles virus. Nature 480:530–533.
21. **Noyce RS, et al.** 2011. Tumor cell marker PVRL4 (nectin 4) is an epithelial cell receptor for measles virus. PLoS Pathog. 7:e1002240. doi:10.1371/journal.ppat.1002240.
22. **Ono N, et al.** 2001. Measles viruses on throat swabs from measles patients use signaling lymphocytic activation molecule (CDw150) but not CD46 as a cellular receptor. J. Virol. 75:4399–4401.
23. **Pasquinelli V, et al.** 2004. Expression of signaling lymphocytic activation molecule-associated protein interrupts IFN-gamma production in human tuberculosis. J. Immunol. 172:1177–1185.
24. **Permar SR, et al.** 2007. Clinical measles after measles virus challenge in simian immunodeficiency virus-infected measles virus-vaccinated rhesus monkeys.. J. Infect. Dis. 196:1784–1793.
25. **Shen A, et al.** 2007. Novel pathway for induction of latent virus from resting $CD4^+$ T cells in the simian immunodeficiency virus/macaque model of human immunodeficiency virus type 1 latency.. J. Virol. 81: 1660–1670.
26. **Takeda M, et al.** 2006. Generation of measles virus with a segmented RNA genome. J. Virol. 80:4242–4248.
27. **Tsunetsugu-Yokota Y, et al.** 1997. Efficient virus transmission from dendritic cells to CD4+ T cells in response to antigen depends on close contact through adhesion molecules. Virology 239:259–268.
28. **Vuorinen T, Peri P, Vainionpaa R.** 2003. Measles virus induces apoptosis in uninfected bystander T cells and leads to granzyme B and caspase activation in peripheral blood mononuclear cell cultures. Eur. J. Clin. Invest. 33:434–442.
29. **Yamamoto T, et al.** 2009. Selective transmission of R5 HIV-1 over X4 HIV-1 at the dendritic cell-T cell infectious synapse is determined by the T cell activation state. PLoS Pathog. 5:e1000279. doi:10.1371/journal.ppat.1000279.

JVI
Journals.ASM.org

# Nectin4 Is an Epithelial Cell Receptor for Canine Distemper Virus and Involved in Neurovirulence

**Watanyoo Pratakpiriya,[a,b] Fumio Seki,[c] Noriyuki Otsuki,[c] Kouji Sakai,[c] Hideo Fukuhara,[d] Hiromu Katamoto,[e] Takuya Hirai,[a] Katsumi Maenaka,[d] Somporn Techangamsuwan,[b] Nguyen Thi Lan,[f] Makoto Takeda,[c] and Ryoji Yamaguchi[a]**

Department of Veterinary Pathology, Faculty of Agriculture, University of Miyazaki, Miyazaki, Japan[a]; Department of Pathology, Faculty of Veterinary Science, Chulalongkorn University, Bangkok, Thailand[b]; Department of Virology 3, National Institute of Infectious Diseases, Tokyo, Japan[c]; Laboratory of Biomolecular Science, Faculty of Pharmaceutical Sciences, Hokkaido University, Sapporo, Japan[d]; Department of Veterinary Internal Medicine, Faculty of Agriculture, University of Miyazaki, Miyazaki, Japan[e]; and Department of Pathology, Faculty of Veterinary Medicine, Hanoi University of Agriculture, Hanoi, Vietnam[f]

**Canine distemper virus (CDV) uses signaling lymphocyte activation molecule (SLAM), expressed on immune cells, as a receptor. However, epithelial and neural cells are also affected by CDV *in vivo*. Wild-type CDV strains showed efficient replication with syncytia in Vero cells expressing dog nectin4, and the infection was blocked by an anti-nectin4 antibody. In dogs with distemper, CDV antigen was preferentially detected in nectin4-positive neurons and epithelial cells, suggesting that nectin4 is an epithelial cell receptor for CDV and also involved in its neurovirulence.**

Distemper is a severe infectious disease that mainly affects dogs and other canids (5). The causative agent is canine distemper virus (CDV), which is closely related to measles virus (MV) (23). CDV belongs to the genus *Morbillivirus* in the family *Paramyxoviridae* and possesses a single-stranded negative-sense RNA genome encoding six structural and two nonstructural proteins (23). Two surface glycoproteins, H and F, play key roles in virus entry. The H protein is responsible for the receptor binding, and the F protein mediates membrane fusion. Signaling lymphocyte activation molecule (SLAM) expressed on cells of the immune system is a receptor for CDV (16). SLAM serves as a common receptor for morbilliviruses (1). Using SLAM as a receptor, CDV primarily replicates in lymphocytes and macrophages in the respiratory tract and then disseminates throughout the body (22). However, SLAM-negative cells in epithelia and the central nervous system (CNS) are also affected by CDV *in vivo* (2, 21). Recently, nectin4 was identified as an epithelial cell receptor for MV (13, 14). In humans, nectin4 is expressed mainly in the placenta and, to lesser extents, in the tonsil, oral mucosa, trachea, esophagus, nasopharynx, prostate, lung, and stomach (13, 14, 20). Although MV also exhibits neurovirulence and causes a persistent infection of the CNS, subacute sclerosing panencephalitis (SSPE), neither SLAM nor nectin4 was detected in neural cells of the human CNS (13, 14, 20). The frequency of SSPE is 1/5,000 to 1/100,000 in reported cases of acute measles (3, 19). In contrast, acute infection of animals with CDV is often accompanied by severe neurological manifestations, which are rarely seen in patients with acute measles (2, 21). The aim of the present study was to elucidate the roles for nectin4 in CDV pathogenesis, including its neurovirulence.

Six wild-type CDV strains (Ac96I, 007Lm, Th12, M24Cr, 55L, and 82Con) isolated from dogs with distemper by using Vero.DogSLAMtag cells were employed in the present study. Some of these strains were reported previously (7, 8, 10). Within 2 days after infection, they all induced syncytia in Vero cells constitutively expressing dog nectin4 (Vero/dNectin4), but not in the parental Vero cells (Fig. 1A, B, and C). The formation of syncytia was completely blocked by 20 μg/ml of a goat anti-human nectin4 polyclonal antibody (R&D Systems) and clearly reduced by 10 μg/ml of the antibody (Fig. 1D). Production of infectious virus particles was inhibited by the anti-nectin4 antibody in a dose-dependent manner (Fig. 1E). Although CDV replicated poorly in Vero cells, it replicated efficiently in Vero/dNectin4 cells (Fig. 1F), as observed in Vero.DogSLAMtag cells. CDV produced plaques in Vero.DogSLAMtag and Vero/dNectin4 cells, but not in the parental Vero cells, although PFU were reduced by ~3-fold in Vero/dNectin4 cells compared to Vero.DogSLAMtag cells (Fig. 1G). The size of plaques was also smaller in Vero/dNectin4 cells than in Vero.DogSLAMtag cells (Fig. 1G). These findings indicate that dog nectin4 functions as a CDV receptor, similar to the case with MV (13, 14).

Seven dogs with distemper were necropsied, and tissues were subjected to histopathological analyses. Hematoxylin and eosin staining of the tissue samples revealed pathognomonic changes with CDV infection, including lymphoid depletion, catarrhal enteritis, bronchointerstitial pneumonia, and nonsuppurative encephalitis (data not shown) (9). Eosinophilic intracytoplasmic and intranuclear inclusion bodies were observed in the brain, lymphoid organs, and lung (data not shown). Immunohistochemical double staining for CDV antigen and nectin4 was conducted in two ways. In the first method, CDV antigen was stained pink by Fast red II and nectin4 was stained brown by diaminobenzidine (Fig. 2). In the second method, CDV antigen and nectin4 were labeled with the red fluorescent probe Alexa Fluor 594 and green fluorescent probe Alexa Fluor 488 (Fig. 3). Nectin4 was expressed in all epithelia of the lung, kidney, intestine, and urinary bladder (Fig. 2A to D and 3A to C and data not shown). CDV antigen was detected in accordance with some of the nectin4-positive epithelial cells (Fig. 2A to D and 3A to C and data not shown). Impor-

**Received** 3 April 2012 **Accepted** 25 June 2012
**Published ahead of print** 3 July 2012
Address correspondence to Ryoji Yamaguchi, a0d402u@cc.miyazaki-u.ac.jp.
W.P and F.S. contributed equally to this work.

doi:10.1128/JVI.00824-12

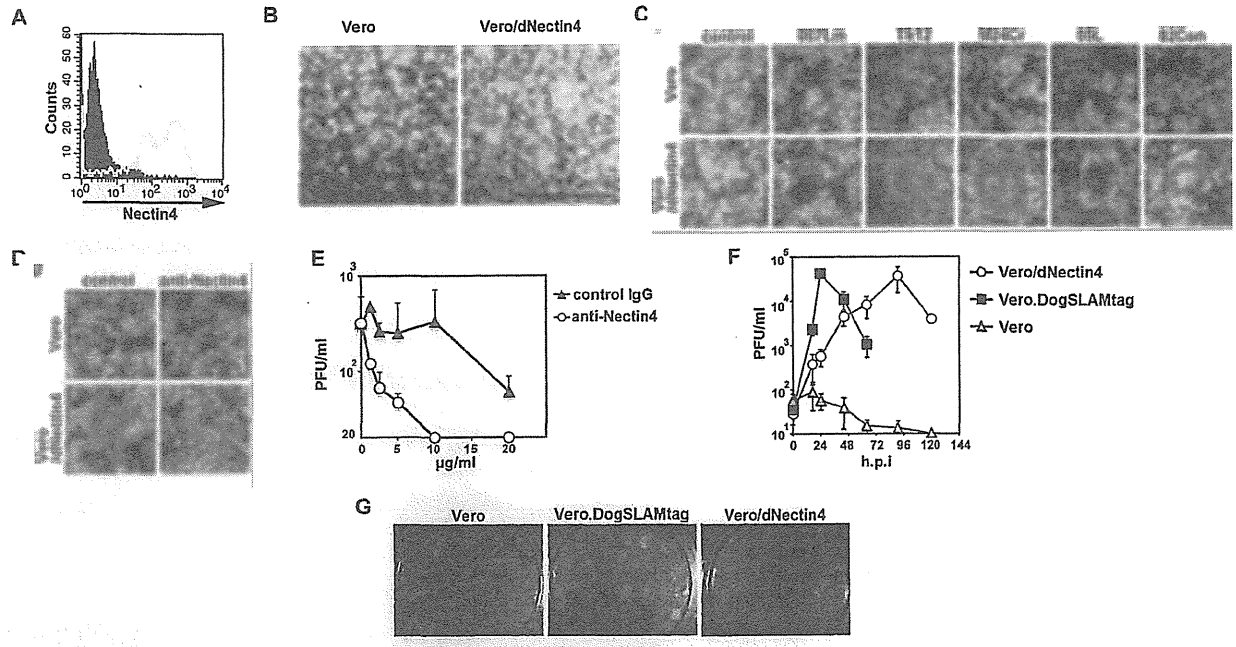


FIG 1 Infection of Vero/dNectin4 cells with CDV. (A) Vero/dNectin4 (gray empty profile) and parental Vero (filled black profile) cells were stained with a goat anti-human nectin4 polyclonal antibody (R&D Systems), followed by staining with Alexa Fluor 488-conjugated anti-goat IgG. (B) Vero/dNectin4 (right panel) and parental Vero (left panel) cells were infected with the Ac96I strain. At 48 h postinfection, the cells were observed under a phase-contrast microscope. Bar, 1 mm. (C) Vero/dNectin4 (lower panels) and parental Vero (upper panels) cells were infected with wild-type strains of CDV (007Lm, Th12, M24Cr, 55L, or 82Con) or left uninfected (control). At 48 h postinfection, the cells were observed under a phase-contrast microscope. (D) Vero/dNectin4 (lower panels) and parental Vero (upper panels) cells were infected with the wild-type Ac96I CDV strain in the presence (anti-Nectin4) or absence (control) of the goat anti-human nectin4 polyclonal antibody. At 48 h postinfection, the cells were observed under a phase-contrast microscope. (E) Vero/dNectin4 cells pretreated with increasing concentrations of anti-Nectin4 antibody or control IgG were infected with 1,000 PFU of strain Ac96I and cultured with the same concentrations of the antibody or control IgG. At 48 h postinfection, the virus titers of the supernatants were determined in plaque assays. (F) Vero/dNectin4, Vero.DogSLAMtag, and parental Vero cells were infected with the wild-type Ac96I CDV strain at a multiplicity of infection of 0.05. At various time intervals, the virus titers were determined in plaque assays. (F) Vero/dNectin4 (right panel), Vero.DogSLAMtag (middle panel), and the parental Vero (left panel) cells in 12 well-cluster plates were infected with the wild-type Th12 strain and overlaid with medium containing 1% agarose. At 7 days postinfection, the plaques were observed under a stereoscope.

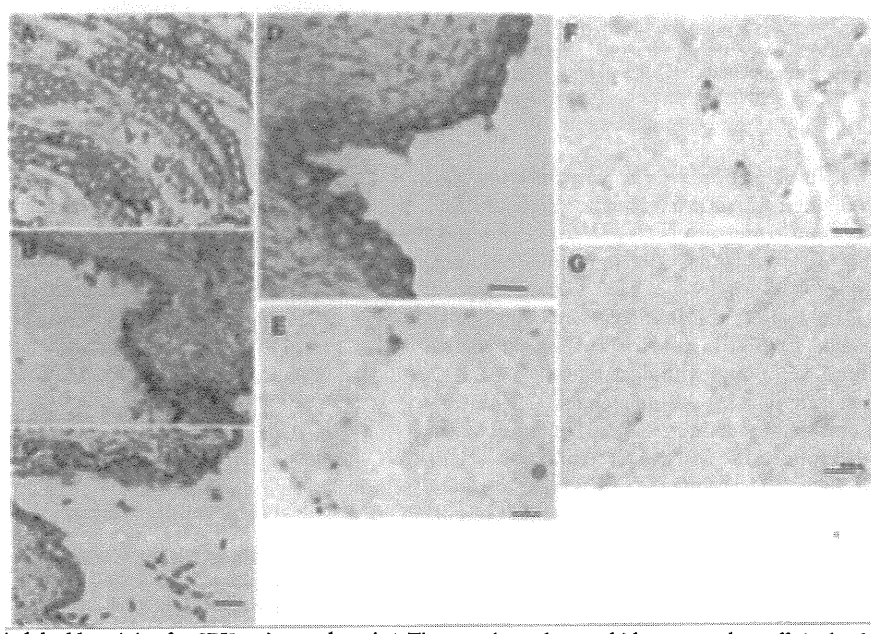

FIG 2 Immunohistochemical double staining for CDV antigen and nectin4. Tissue sections of 2-μm thickness were deparaffinized, rehydrated, and subjected to heat-induced antigen retrieval before incubation with antibodies. Subsequently, blocking of endogenous peroxidase was performed. The tissue sections were then incubated with a mouse monoclonal anti-CDV antibody (Adtec, Japan) and a goat anti-nectin4 polyclonal antibody (R&D Systems). Using an EnVision kit (Dako) and 3′,3-diaminobenzidine (Sigma), CDV antigen and nectin4 were visualized (pink and brown staining, respectively), according to the manufacturer's protocol. (A) Intestine; (B) lung; (C) renal pelvis; (D) urinary bladder; (E) cerebellum; (F) cerebrum; (G) midbrain. Bars, 20 μm (A, B, D, E, and F) or 40 μm (C and G).

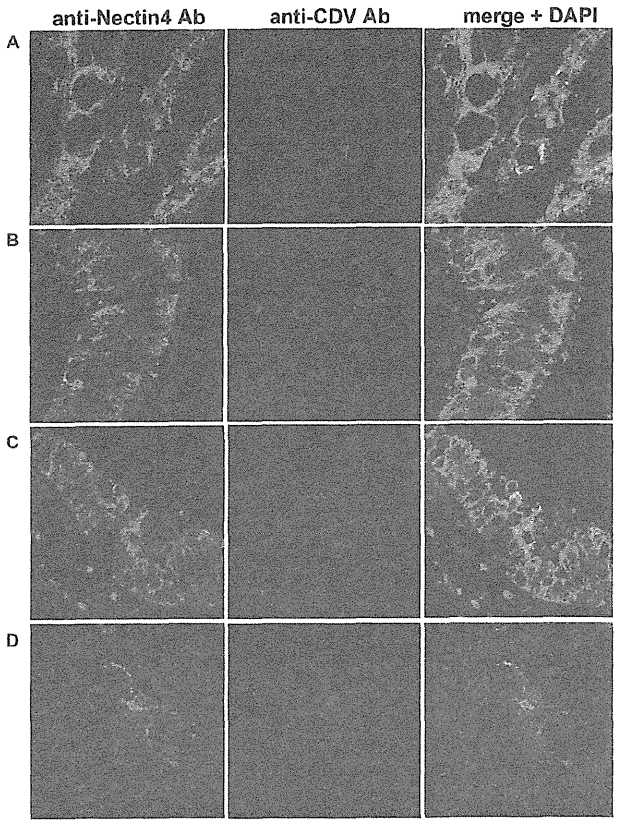


FIG 3 Immunofluorescence double staining for CDV antigen and nectin4. Tissue sections of 2-μm thickness were deparaffinized, rehydrated, and subjected to heat-induced antigen retrieval before incubation with antibodies. CDV antigen was stained with a mouse anti-CDV monoclonal antibody (Adtec, Japan) and Alexa Fluor 594-conjugated secondary (red) antibody. Nectin4 was stained with a goat anti-nectin4 polyclonal antibody (R&D Systems) and Alexa Fluor 488-conjugated secondary antibody (green). Nuclei were counterstained with 4′,6-diamidino-2-phenylindole (DAPI; blue). (A) Intestine; (B and C) lung; (D) brain.

tantly, and in contrast to the reports for humans, nectin4 was detected in the brain of dogs, and CDV antigen was preferentially detected in the nectin4-positive neurons (Fig. 2E to G and 3D). These findings suggest that nectin4 may contribute to infection of the CNS with CDV.

Although SLAM is not expressed in epithelial and neural cells, CDV antigen is often detected at high levels in the epithelia of various organs and the CNS of dogs with distemper (21). Several candidate molecules that support SLAM-independent CDV infection have previously been reported. Fujita et al. (6) reported that a heparin-like molecule supports the entry of CDV into cells of the human embryonic kidney 293 cell line. CD9 has also been described to support cell-to-cell fusion by CDV (12, 15, 17). A recent study further showed that chicken embryo fibroblasts and monkey kidney Vero cells express unidentified receptor molecules for CDV with molecular masses of 57 and 42 kDa, respectively (4). However, that study did not provide a solid conclusion for the *in vivo* epithelial and neural receptors of CDV (4, 6, 12, 15, 17). For MV, a breakthrough came with the identification of nectin4 as an epithelial receptor for the virus, implying an efficient mechanism for MV transmission, although the mechanisms for MV infection of neural cells remained unclear (13, 14). In the present study, we investigated CDV as a model of morbillivirus infection of the CNS, since the virus often causes severe infection of the CNS in infected animals (21). Our data demonstrated that dog canine nectin4 functions as a CDV receptor and is expressed in neural cells of the brain as well as the epithelia of various organs. In the brain, nectin4-positive neurons were preferentially targeted by CDV. Therefore, CDV infection of the CNS could be partly explained by the knowledge that dog canine nectin4 acts as a receptor for CDV. Like SLAM, nectin4 seems to be a common receptor for morbilliviruses, because critical residues of the H protein required for nectin4 binding are highly conserved among morbilliviruses (11, 18). Thus, the findings in the present study contribute to our understanding of the pathogenesis of CDV, and possibly other morbilliviruses.

## ACKNOWLEDGMENTS

We thank Y. Yanagi for providing the Vero.DogSLAMtag cells.

This work was supported by grants from the Ministry of Education, Culture, Sports, Science and Technology, the Ministry of Health, Labor and Welfare of Japan, and the Takeda Science Foundation. W. Pratakpiriya was supported by a granted Chulalongkorn University tuition fee scholarship.

## REFERENCES

1. **Adombi CM, et al.** 2011. Monkey CV1 cell line expressing the sheep-goat SLAM protein: a highly sensitive cell line for the isolation of peste des petits ruminants virus from pathological specimens. J. Virol. Methods 173:306–313.
2. **Appel MJ, Summers BA.** 1995. Pathogenicity of morbilliviruses for terrestrial carnivores. Vet. Microbiol. 44:187–191.
3. **Bellini WJ, et al.** 2005. Subacute sclerosing panencephalitis: more cases of this fatal disease are prevented by measles immunization than was previously recognized. J. Infect. Dis. 192:1686–1693.
4. **Chen J, Liang X, Chen PF.** 2011. Canine distemper virus utilizes different receptors to infect chicken embryo fibroblasts and Vero cells. Virol. Sin. 26:139–145.
5. **Deem SL, Spelman LH, Yates RA, Montali RJ.** 2000. Canine distemper in terrestrial carnivores: a review. J. Zoo Wildl. Med. 31:441–451.
6. **Fujita K, et al.** 2007. Host range and receptor utilization of canine distemper virus analyzed by recombinant viruses: involvement of heparin-like molecule in CDV infection. Virology 359:324–335.
7. **Lan NT, Yamaguchi R, Hirai T, Kai K, Morishita K.** 2009. Relationship between growth behavior in Vero cells and the molecular characteristics of recent isolated classified in the Asia 1 and 2 groups of canine distemper virus. J. Vet. Med. Sci. 71:457–461.
8. **Lan NT, et al.** 2006. Comparative analyses of canine distemper viral isolates from clinical cases of canine distemper in vaccinated dogs. Vet. Microbiol. 115:32–42.
9. **Lan NT, et al.** 2009. First isolation and characterization of canine distemper virus in Vietnam with the immunohistochemical examination of the dog. J. Vet. Med. Sci. 71:155–162.
10. **Lan NT, Yamaguchi R, Uchida K, Sugano S, Tateyama S.** 2005. Growth profiles of recent canine distemper isolates on Vero cells expressing canine signalling lymphocyte activation molecule (SLAM). J. Comp. Pathol. 133:77–81.
11. **Leonard VH, et al.** 2008. Measles virus blind to its epithelial cell receptor remains virulent in rhesus monkeys but cannot cross the airway epithelium and is not shed. J. Clin. Invest. 118:2448–2458.
12. **Loffler S, et al.** 1997. CD9, a tetraspan transmembrane protein, renders cells susceptible to canine distemper virus. J. Virol. 71:42–49.
13. **Muhlebach MD, et al.** 2011. Adherens junction protein nectin-4 is the epithelial receptor for measles virus. Nature 480:530–533.
14. **Noyce RS, et al.** 2011. Tumor cell marker PVRL4 (nectin 4) is an epithelial cell receptor for measles virus. PLoS Pathog. 7:e1002240. doi:10.1371/journal.ppat.1002240.
15. **Schmid E, et al.** 2000. Antibodies to CD9, a tetraspan transmembrane protein, inhibit canine distemper virus-induced cell-cell fusion but not virus-cell fusion. J. Virol. 74:7554–7561.
16. **Seki F, Ono N, Yamaguchi R, Yanagi Y.** 2003. Efficient isolation of wild strains

of canine distemper virus in Vero cells expressing canine SLAM (CD150) and their adaptability to marmoset B95a cells. J. Virol. 77:9943–9950.
17. **Singethan K, et al.** 2006. CD9-dependent regulation of canine distemper virus-induced cell-cell fusion segregates with the extracellular domain of the haemagglutinin. J. Gen. Virol. 87:1635–1642.
18. **Tahara M, et al.** 2008. Measles virus infects both polarized epithelial and immune cells by using distinctive receptor-binding sites on its hemagglutinin. J. Virol. 82:4630–4637.
19. **Takasu T, et al.** 2003. A continuing high incidence of subacute sclerosing panencephalitis (SSPE) in the Eastern Highlands of Papua New Guinea. Epidemiol. Infect. 131:887–898.
20. **Takeda M, Tahara M, Nagata N, Seki F.** 2011. Wild-type measles virus is intrinsically dual-tropic. Front. Microbiol. 2:279.
21. **van Moll P, Alldinger S, Baumgartner W, Adami M.** 1995. Distemper in wild carnivores: an epidemiological, histological and immunocytochemical study. Vet. Microbiol. 44:193–199.
22. **von Messling V, Milosevic D, Cattaneo R.** 2004. Tropism illuminated: lymphocyte-based pathways blazed by lethal morbillivirus through the host immune system. Proc. Natl. Acad. Sci. U. S. A. 101:14216–14221.
23. **Wang L-F, et al.** 2012. Family *Paramyxoviridae*, p 672–685. *In* King AMQ, Adams MJ, Carstens EB, Lefkowitz EJ (ed), Virus taxonomy, 9th ed. Elsevier Academic Press, London, United Kingdom.

PLOS | ONE

# Molecular Evolution of Hemagglutinin (*H*) Gene in Measles Virus Genotypes D3, D5, D9, and H1

**Mika Saitoh[1], Makoto Takeda[2], Koichi Gotoh[1], Fumihiko Takeuchi[3], Tsuyoshi Sekizuka[3], Makoto Kuroda[3], Katsumi Mizuta[4], Akihide Ryo[5], Ryota Tanaka[6], Haruyuki Ishii[7], Hayato Takada[1], Kunihisa Kozawa[1], Ayako Yoshida[8], Masahiro Noda[9], Nobuhiko Okabe[9], Hirokazu Kimura[1,9]***

**1** Gunma Prefectural Institute of Public Health and Environmental Sciences, Maebashi-shi, Gunma, Japan, **2** Department of Virology III, National Institute of Infectious Diseases, Musashimurayama-shi, Tokyo, Japan, **3** Pathogen Genomics Center, National Institute of Infectious Diseases, Shinjuku-ku, Tokyo, Japan, **4** Yamagata Prefectural Institute of Public Health, Yamagata-shi, Yamagata, Japan, **5** Department of Molecular Biodefence Research, Yokohama City University Graduate School of Medicine, Yokohama-shi, Kanagawa, Japan, **6** Department of Surgery, Institute of Medical Sciences, Kyorin University, Mitaka-shi, Tokyo, Japan, **7** Department of Respiratory Medicine, Kyorin University, School of Medicine, Mitaka-shi, Tokyo, Japan, **8** Aomori Prefectural Institute of Public Health and Environment, Aomori-shi, Aomori, Japan, **9** Infectious Disease Surveillance Center, National Institute of Infectious Diseases, Musashimurayama-shi, Tokyo, Japan

## Abstract

We studied the molecular evolution of *H* gene in four prevalent Asian genotypes (D3, D5, D9, and H1) of measles virus (MeV). We estimated the evolutionary time scale of the gene by the Bayesian Markov Chain Monte Carlo (MCMC) method. In addition, we predicted the changes in structure of H protein due to selective pressures. The phylogenetic tree showed that the first division of these genotypes occurred around 1931, and further division of each type in the 1960–1970s resulted in four genotypes. The rate of molecular evolution was relatively slow ($5.57\times10^{-4}$ substitutions per site per year). Only two positively selected sites (F476L and Q575K) were identified in H protein, although these substitutions might not have imparted significant changes to the structure of the protein or the epitopes for phylactic antibodies. The results suggested that the prevalent Asian MeV genotypes were generated over approximately 30–40 years and H protein was well conserved.

**Citation:** Saitoh M, Takeda M, Gotoh K, Takeuchi F, Sekizuka T, et al. (2012) Molecular Evolution of Hemagglutinin (*H*) Gene in Measles Virus Genotypes D3, D5, D9, and H1. PLoS ONE 7(11): e50660. doi:10.1371/journal.pone.0050660

**Editor:** Paul J. Planet, Columbia University, United States of America

**Received** May 18, 2012; **Accepted** October 25, 2012; **Published** November 29, 2012



**Funding:** No current external funding sources for this study.

**Competing Interests:** The authors have declared that no competing interests exist.

* E-mail: kimhiro@nih.go.jp

## Introduction

Measles virus (MeV) of genus *Morbillivirus* and family *Paramyxoviridae* causes acute and highly contagious measles infection in humans [1,2]. Since the year 2000, the number of patients in many countries with measles has continued to decrease due to widespread measles immunization programs [3]. Nevertheless, an estimated 300,000 cases were reported and 140,000 young children died from measles globally in 2010 (Media Centre. Measles. World Health Organization. http://www.who.int/mediacentre/factsheets/fs286/en/index.html). Thus, the World Health Organization has focused on the infection as an eliminative disease.

Many genotypes of MeV have been identified, although the virus may be confirmed as a monoserotype [1,2]. Interestingly, there are associations between the prevalence of each genotype and geographical area [4]. For example, genotypes D4 and D6 are mainly detected in European countries, while genotypes D3, D5, D9, and H1 are mainly detected in Asian countries [4]. At present, in some countries that have eliminated measles, a small numbers of cases are caused by a number of different genotypes that reflect various sources of imported viruses [2]. The MeV genome encodes some essential structural proteins such as hemagglutinin (H) and fusion (F) proteins [1]. The H protein generally regulates viral adsorption and entry, and that of the vaccine strains shows hemagglutinin activity as well [1]. The neutralizing antibodies against H protein act as protective antibodies in MeV infection. In addition, recent studies have shown the detailed structure of the H protein and the epitopes for the neutralizing antibodies [5,6]. Such antigenic changes may occur through positively selected amino acid substitutions due to selection pressures in the host. Indeed, attachment glycoprotein (G protein), an essential antigen of respiratory syncytial virus, shows frequent positive selections in the epitopes of the protein, whereas no positive selection sites have been found in the HN protein (a major antigen) of human parainfluenza virus type 1 [7,8]. This suggests that the frequency of the positive selection sites differs among the major antigens of these viruses, even though the viruses all belong to the same family, *Paramyxoviridae*. Thus, it may be important to analyze the molecular evolution of *H* gene in MeV.

The Bayesian Markov Chain Monte Carlo (MCMC) method enables the evolutionary time scale to be estimated [9,10]. Furthermore, detailed changes in H protein structure may be predictive. In the present study we conducted a detailed genetic analysis of the gene and predicted changes in the structure of H protein to gain a better understanding of the evolution of *H* gene in prevalent Asian MeV genotypes (D3, D5, D9, and H1).

## Results

### Phylogenetic Analysis Using the Bayesian MCMC Method on the *H* Coding Region of MeV

The phylogenetic tree constructed using the Bayesian MCMC method with the nucleotide sequences of the *H* gene (1854 nt) for various genotypes (A to H) of MeV is shown in Fig. 1. The year of the first major division in the present tree was estimated as approximately 1931 (95% confidence interval [CI] 1906–1952). The D3, D5, and D9 subdivisions occurred in approximately 1975 (95% CI 1970–1980) and 1977 (95% CI 1972–1982), and the H1 and H2 subdivisions occurred in approximately 1966 (95% CI 1950–1979), resulting in the formation of 4 genotype clusters [D3 (14 strains), D5 (14 strains), D9 (6 strains), and H1 (27 strains)]. Further division of each genotype occurred in approximately 1980 (95% CI 1976–1983) for D3, 1980 (95% CI 1974–1985) for D5, 1987 (95% CI 1980–1993) for D9, and 1977 (95% CI 1968–1984) for H1. The CIs for each node of the phylogenetic tree are expressed as gray bars in Fig. 1. The rate of molecular evolution was estimated from the tree as $5.57\times10^{-4}$ substitutions per site per year (95% CI $4.50\times10^{-4}$–$6.81\times10^{-4}$).

### Analysis of Selective Pressure of *H* Gene in MeV

Selection pressure analysis was performed in the strains of the various genotypes (A to H) in MeV *H* gene, and dN/dS values were calculated by the single likelihood ancestor counting (SLAC), fixed effects likelihood (FEL), and internal fixed effects likelihood (IFEL) methods, significant at the $p<0.05$ level. The global estimate of dN/dS was 0.22 (95% CIs of 0.19–0.24) by SLAC. Estimates of the dN/dS ratio of two codons were detected and two amino acid substitutions were estimated (F476L and Q575K) by the FEL and IFEL methods (Table 1). Negatively selected sites were detected by each of the three methods and 28 codons were identified (Table 1).

### Location of the Two Positively Selected Amino Acid Sites

The two amino acid positions (476 and 575) were shown on the H protein structure [6]. The residues are exposed on the surface (light green and blue, respectively; Fig. 2). Therefore, they may be parts of epitopes, but to date there are no reports showing that the regions containing residues 476 or 575 constitute epitopes (known epitopes are shown in red in Fig. 2). The structural data showed that these residues are located at the bottom and lateral surfaces, respectively, of the H head dimer, and distal from the SLAM-binding site (SLAM is shown in cyan in Fig. 2).

## Discussion

We analyzed the molecular evolution of *H* gene in genotypes D3, D5, D9, and H1 of MeV, which are prevalent in Asian countries including China and Japan. First, we estimated the evolutionary time scale of the gene using the Bayesian MCMC method. The first division of these genotypes in the present tree was estimated as approximately 1931, and each genotype further divided in the 1960–70s, resulting in 4 genotypes. In addition, only two positively selected sites were observed, although these changes might not reflect significant structural changes in H protein. The results suggested that the 4 genotypes were formed over a period of approximately 30–40 years (from approximately 1931 to the 1960–70s) and the structure of the H protein has been well conserved.

MeV genotype D3 was mainly detected in various Western Pacific countries including Japan, Australia, Papua New Guinea, and the Philippines during 1983–2006, and was endemic in Papua New Guinea and possibly the Philippines from 2002–2006 [2,11,12]. The first major division of type D3 was estimated at around 1975, and the ancestral strains further subdivided from around 1980 (Fig. 1). Genotype D5 has been prevalent in Japan, Australia, and Cambodia since 1985 [2,11,12]. Until 2001, both D3 and the D5 genotypes were endemic in Japan. The first major division of type D5 was estimated at around 1975, and extensive branching into two clusters occurred around 1980. Furthermore, it is suggested that the ancestral strains have undergone further divisions from around 1990. Genotype D9 was first described after importation to Australia from Indonesia in 1999 and was associated with an outbreak in Japan in 2004 [2,11,12]. The strains detected in Japan and France in the mid-2000s had diverged in approximately 1990 from the strains detected in Australia in 1999. Genotype H1, detected during the large measles epidemic in Korea in 2000–2001, has been prevalent in China, Japan, Korea, Vietnam, and Australia since 1993 and is mainly associated with transmission within China or in importations from China [2,11,12]. This genotype diverged into plural clusters after 1977. The Korean strain detected in Korea in 2000 evolved from one Chinese strain clusters in about 1995. The results showed that the Asian prevalent MeV genotypes D3, D5, D9, and H1 were generated over approximately 30–40 years, and the ages of the diverged clusters for each genotype could be predicted. In the present study, it is estimated that each genotype, e.g., D3, D5, D9, and H1, was generated from the 1960s to 70s. However, there was a difference in the year that the viruses were generated according to the phylogenetic tree based on the Bayesian MCMC method and the year that they were first detected. For example, the D9 strain was shown to be generated approximately 40 years ago using the phylogenetic tree, while the virus was detected in 1999. This has been seen in other viruses, such as rubella virus [13]. Indeed, Zhu et al. showed that cluster 1 isolates of Chinese genotype 1E rubella virus were collected from 2001 to 2009, while the viruses were estimated to have appeared in 1997 according to the MCMC method. To solve this discrepancy, additional studies are needed.

We analyzed the rate of molecular evolution from the tree as $5.57\times10^{-4}$ substitutions per site per year. The rates of evolution of *H* gene in seasonal influenza virus subtype A and *G* gene in respiratory syncytial virus are estimated at about $10^{-3}$ substitutions per site per year [14,15]. In addition, we reported that the rate of *HN* gene in human parainfluenza virus type 1 is estimated at $7.68\times10^{-4}$ substitutions/site/year [8]. These results suggest that the rate of evolution of *H* gene of MeV may be similar to the rate of *HN* gene of human parainfluenza virus type 1, and their rates of molecular evolution may be relatively slow [8].

We estimated positively and negatively selected sites in the gene by the SLAC, FEL, and IFEL methods. Positive selection shows a survival advantage under the selective constraints that confront the viral population [16]. Negative selection plays an important role in maintaining the long-term stability of biological structures by removing deleterious mutations [16,17]. In this study, two positively selected sites (F476L and Q575K) were found. Woelk et al demonstrated 14 positively selected sites in 50 strains of *H* gene in all genotypes of MeV [18]. Of these, amino acid positions corresponding to 476 and 575 are compatible with our results. Region 463–477 including site 476 and region 561–575 including site 575 react with human sera. Furthermore, region 463–477 is a possible candidate for interaction with the CD46 receptor. In addition, Corey and Iorio have shown that amino acid substitutions at region 473–477 including 476 drastically reduce hemagglutinin activity associated with fusion promotion [19]. In this study, it is suggested that the amino acid substitutions of two

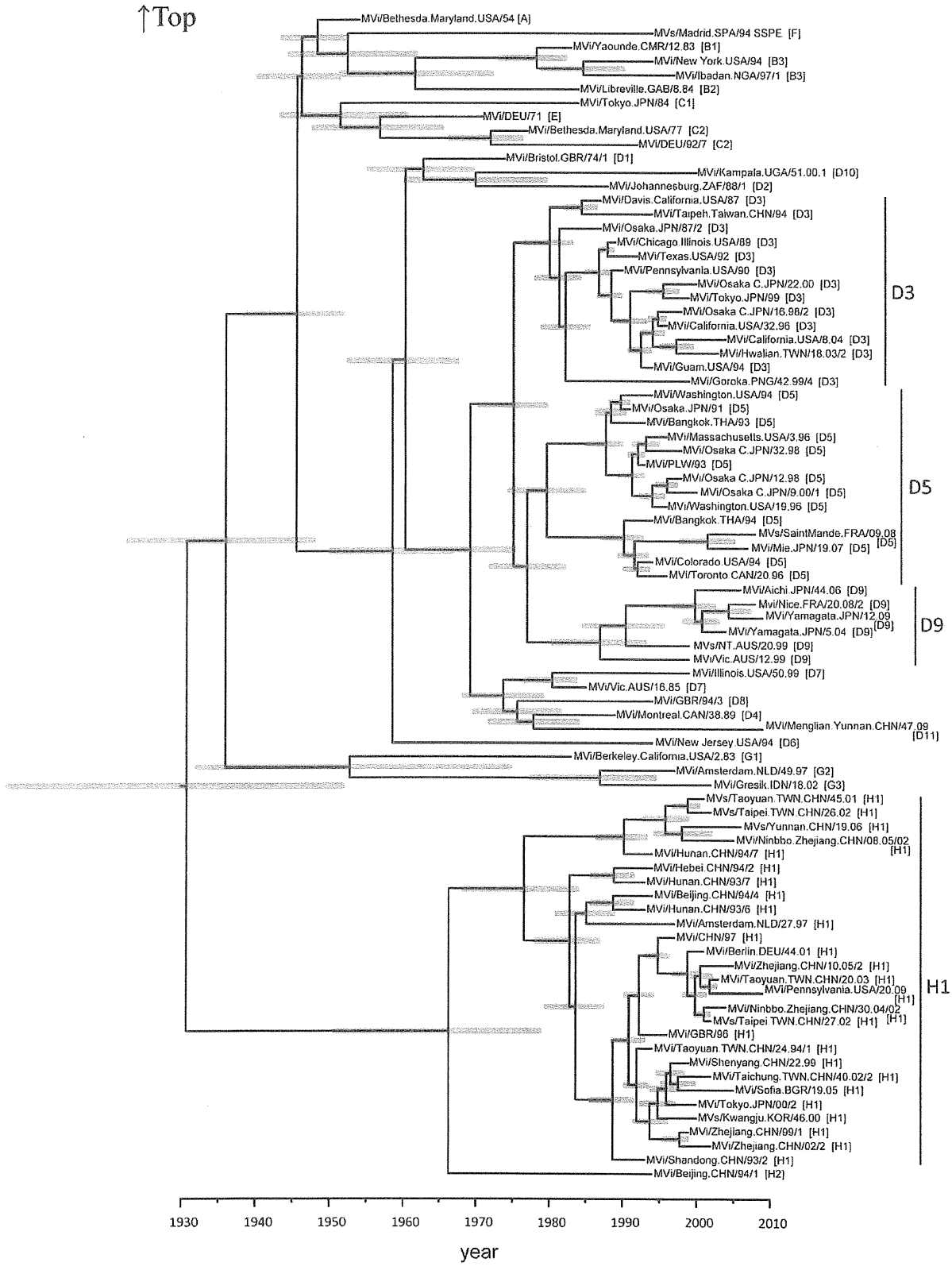
↑Top
MVi/Bethesda.Maryland.USA/54 [A]
MVs/Madrid.SPA/94 SSPE [F]
MVi/Yaounde.CMR/12.83 [B1]
MVi/New York.USA/94 [B3]
MVi/Ibadan.NGA/97/1 [B3]
MVi/Libreville.GAB/8.84 [B2]
MVi/Tokyo.JPN/84 [C1]
MVi/DEU/71 [E]
MVi/Bethesda.Maryland.USA/77 [C2]
MVi/DEU/92/7 [C2]
MVi/Bristol.GBR/74/1 [D1]
MVi/Kampala.UGA/51.00.1 [D10]
MVi/Johannesburg.ZAF/88/1 [D2]
MVi/Davis.California.USA/87 [D3]
MVi/Taipeh.Taiwan.CHN/94 [D3]
MVi/Osaka.JPN/87/2 [D3]
MVi/Chicago.Illinois.USA/89 [D3]
MVi/Texas.USA/92 [D3]
MVi/Pennsylvania.USA/90 [D3]
MVi/Osaka C.JPN/22.00 [D3]
MVi/Tokyo.JPN/99 [D3]
MVi/Osaka C.JPN/16.98/2 [D3]
MVi/California.USA/32.96 [D3]
MVi/California.USA/8.04 [D3]
MVi/Hwalian.TWN/18.03/2 [D3]
MVi/Guam.USA/94 [D3]
MVi/Goroka.PNG/42.99/4 [D3]
D3
MVi/Washington.USA/94 [D5]
MVi/Osaka.JPN/91 [D5]
MVi/Bangkok.THA/93 [D5]
MVi/Massachusetts.USA/3.96 [D5]
MVi/Osaka C.JPN/32.98 [D5]
MVi/PLW/93 [D5]
MVi/Osaka C.JPN/12.98 [D5]
MVi/Osaka C.JPN/9.00/1 [D5]
MVi/Washington.USA/19.96 [D5]
MVi/Bangkok.THA/94 [D5]
MVs/SaintMande.FRA/09.08 [D5]
MVi/Mie.JPN/19.07 [D5]
MVi/Colorado.USA/94 [D5]
MVi/Toronto.CAN/20.96 [D5]
D5
MVi/Aichi.JPN/44.06 [D9]
Mvi/Nice.FRA/20.08/2 [D9]
MVi/Yamagata.JPN/12.09 [D9]
MVi/Yamagata.JPN/5.04 [D9]
MVs/NT.AUS/20.99 [D9]
MVi/Vic.AUS/12.99 [D9]
D9
MVi/Illinois.USA/50.99 [D7]
MVi/Vic.AUS/16.85 [D7]
MVi/GBR/94/3 [D8]
MVi/Montreal.CAN/38.89 [D4]
MVi/Menglian.Yunnan.CHN/47.09 [D11]
MVi/New Jersey.USA/94 [D6]
MVi/Berkeley.California.USA/2.83 [G1]
MVi/Amsterdam.NLD/49.97 [G2]
MVi/Gresik.IDN/18.02 [G3]
MVs/Taoyuan.TWN.CHN/45.01 [H1]
MVs/Taipei.TWN.CHN/26.02 [H1]
MVs/Yunnan.CHN/19.06 [H1]
MVi/Ninbbo.Zhejiang.CHN/08.05/02 [H1]
MVi/Hunan.CHN/94/7 [H1]
MVi/Hebei.CHN/94/2 [H1]
MVi/Hunan.CHN/93/7 [H1]
MVi/Beijing.CHN/94/4 [H1]
MVi/Hunan.CHN/93/6 [H1]
MVi/Amsterdam.NLD/27.97 [H1]
MVi/CHN/97 [H1]
MVi/Berlin.DEU/44.01 [H1]
MVi/Zhejiang.CHN/10.05/2 [H1]
MVi/Taoyuan.TWN.CHN/20.03 [H1]
MVi/Pennsylvania.USA/20.09 [H1]
MVi/Ninbbo.Zhejiang.CHN/30.04/02 [H1]
MVs/Taipei.TWN.CHN/27.02 [H1]
MVi/GBR/96 [H1]
MVi/Taoyuan.TWN.CHN/24.94/1 [H1]
MVi/Shenyang.CHN/22.99 [H1]
MVi/Taichung.TWN.CHN/40.02/2 [H1]
MVi/Sofia.BGR/19.05 [H1]
MVi/Tokyo.JPN/00/2 [H1]
MVs/Kwangju.KOR/46.00 [H1]
MVi/Zhejiang.CHN/99/1 [H1]
MVi/Zhejiang.CHN/02/2 [H1]
MVi/Shandong.CHN/93/2 [H1]
MVi/Beijing.CHN/94/1 [H2]
H1
1930
1940
1950
1960
1970
1980
1990
2000
2010
year

**Figure 1. Phylogenetic tree of *H* gene by Bayesian Markov Chain Monte Carlo (MCMC) method.** The MCMC tree was based on the full nucleotide sequence of *H* gene (1854 nt) visualized in FigTree. The branch length reflects the evolutionary rate of individual sequences and their reconstructed ancestors. Gray bars indicate 95% confidence intervals for the estimated year. MeV strains were named according to WHO standard nomenclature. The strain names provide following information. MVi: sequence derived from RNA extracted from measles virus isolate in cell culture, MVs: sequence derived from RNA extracted from clinical material/city or province and country: use ISO-3 letter designation/date of onset of rash by epidemiological week and year, and isolate or sequence numbers/genotype in square brackets.
doi:10.1371/journal.pone.0050660.g001

positively selected sites share these particular abilities in MeV *H* gene. Twenty- eight negatively selected sites were found (Table 1). These sites may be optimized biological structures, thus further analysis of the biological properties of H glycoprotein in MeV is required. In addition, it may be important to make a distinction between the branched year of the viruses on a phylogenetic tree and the nucleotide and amino acid substitutions as positive selection. Although this question could not be elucidated in the present study, further studies regarding these relationships are needed.

Finally, we predicted the changes of the epitopes [5,6] for neutralizing antibodies against H protein by substitutions of the amino acid due to positive selection pressure. The amino acid changes at positively selected sites may confer an advantage to MeV in terms of transmission. The residues at amino acid positions 476 and 575 are exposed on the surface, but are located distal from receptor binding site and unrelated to known neutralizing epitopes. Therefore, the amino acid substitutions at these positions may not significantly affect the efficacy of humoral immunity against MeV. These data suggested that in these several decades none of the amino acid substitutions on the epitopes succeeded to give MeV better fitness in nature significantly. These observations could provide a rationale for the high efficacy of currently used MeV vaccines against all MeV strains circulating. In conclusion, it suggested that the prevalent Asian MeV genotypes were generated over approximately 30–40 years and H protein was well conserved. As an essential molecule of these viruses, further analysis of the biological properties of H glycoprotein in MeV is required. Thus, additional and larger molecular epidemiological studies are required to give better understanding of the etiology of MeV.

## Materials and Methods

### Strains

We comprehensively collected total 162 strains of various genotypes of *H* gene sequence (1854 nt), such as 23 reference strains (genotypes A, B1 to B3, C1, C2, D1, D2, D4, D6 to D8, D10, D11, E, F, G1 to 3, and H2 [2]) and Asian-prevalent genotype strains, including the reference strains (D3, 37 strains; D5, 34 strains; D9. 11 strains; and H1, 57 strains), from MeaNS (http://www.hpa-bioinformatics.org.uk/Measles/Public/Web_Front/main.php) [20]. Their sequences correspond to positions 21–1874 (1854 nt) of MVi/Chicago.Illinois.USA/89 (reference strain for genotype D3) (GenBank accession number M81895). The MeV sequences were aligned using the ClustalW web server (http://www.ddbj.nig.ac.jp/index-j.html).

### Phylogenetic Analysis by the Bayesian MCMC Method

Using all of the present strains to estimate the rate of molecular evolution (and hence a time scale) and evolutionary relationships, phylogenetic analyses were performed using the Bayesian MCMC method in the BEAST program (version 1.7.2) [21]. The time of the most recent common ancestor (*t*MRCA) with a 95% highest posterior density (HPD) was estimated by Bayesian molecular dating as described previously [9,10]. The MeV sequences were aligned using the ClustalW web server (http://www.ddbj.nig.ac.jp/index-j.html). We removed the identical sequences from within the MeV *H* coding region of the genotype strains. The dataset was

**Table 1.** Positive and negative selection sites in MeV H coding region in the present study.

| **Positive selection sites.** | | | |
|---|---|---|---|
| **aa position** | **Change** | **†FEL** | **††IFEL** |
| 220V | T or I | | * |
| 282N | K or H or D | | * |
| 235E and G | G or E or A | * | |
| 285S | G or N | | * |
| 451V | E or M or A | | * |
| 476F | L | * | * |
| 546S | G | * | |
| 575Q | K | * | * |
| **Negative selection sites** | | | |
| **aa common position** | | **†FEL** | **††IFEL** |
| 3P,7R,13K,14D,16P,90D,209Y,228Y,237P,242K,259V,297A,374D,388G,400A,401P,487I,489E,492E,515V,538V,541Y,548S,563P,588S,606C,611E,612D | | 131sites | 28sites |

$p<0.05$.
†FEL: Fixed effects likelihood.
††IFEL: International fixed effects likelihood.
doi:10.1371/journal.pone.0050660.t001

↑Top

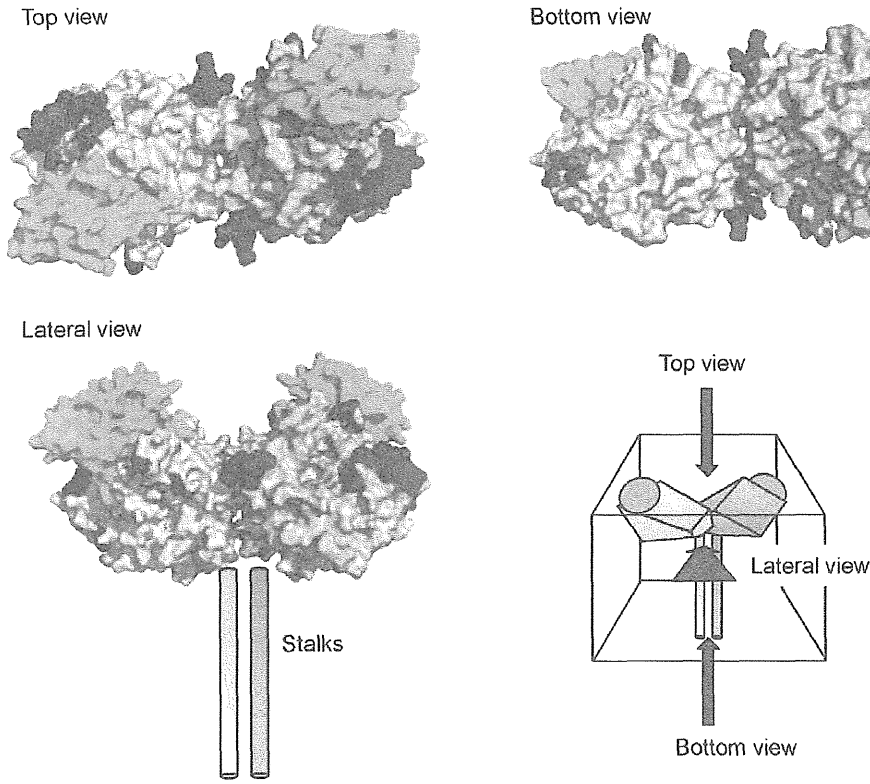


**Figure 2. The predicted structure of H protein in MeV.** The H head dimers are shown from the top, bottom, and lateral angles. Each monomer is shown in gray or orange. Residues reported to constitute epitopes are shown in red. SLAM is shown in cyan. Positively selected amino acid sites, 476 and 575, are shown in light green and blue, respectively.
doi:10.1371/journal.pone.0050660.g002

analyzed under a lognormal relaxed uncorrelated clock using the general time reversible (GTR) model with the gamma distributed rates across sites (GTR+Γ) model selected by the KAKUSAN4 program (version 4.0). The MCMC chain was run for 30,000,000 steps and sampled every 1,000 steps. Uncertainty in the estimates was indicated by the 95% HPD intervals. The parameter outputs generated by the Bayesian MCMC runs and convergence on the basis of the effective sampling size after a 10% burn-in were analyzed using the TRACER program (version 1.5). The trees were summarized in a target tree using the Tree Annotator program (version 1.7.2) by choosing the tree with the maximum posterior probabilities after a 10% burn-in. The phylogenetic tree was viewed in FigTree (version 1.3.1; available at: http://beast.bio.ed.ac.uk). Next, to understand the phylogenetic tree easily, we selected and removed the sequences with high homogeneity and identical isolation years in each cluster of the tree. As a result, the present phylogenetic tree included 23 genotypes of the reference strains and the Asian-prevalent strains, including the reference strains (14 strains of D3, 14 strains of D5, 6 strains of D9, and 27 strains of H1).

## Selective Pressures Analysis

To evaluate selective pressures on the *H* coding regions among all MeV strains, the rates of synonymous (dS) and non-synonymous (dN) changes at amino acid sites were estimated by conservative SLAC, FEL, and IFEL methods using ML available on the Datamonkey webserver (http://www.datamonkey.org/) [22]. The SLAC method is suitable for fast likelihood-based "counting methods" that employ either a single most likely ancestral reconstruction, weighted across all possible ancestral reconstructions, or sampling from ancestral reconstructions. The FEL method directly estimates dN and dS substitution rates at each site. The IFEL method is tested for only along internal branches of the phylogeny in the same manner. To examine the dN and dS rates, these methods were performed incorporating the GTR model of nucleotide substitution and the phylogenetic tree deduced using the NJ method. The dN/dS values of each codon and branch of the present phylogenetic tree were assessed as described previously [23]. Positive (dN>dS) and negative (dN<dS) selections were predicted using the *p*-value [23].

### Prediction of Epitopes for Neutralizing Antibody Against MeV H Protein Based on the Deduced Amino Acid Substitutions

To clarify the location of substituted amino acids on the H protein, we mapped the positively and negatively selected sites as previously described [5,6]. Figures were produced using PyMOL (DeLano Scientific LLC, Palo Alto, CA, USA. http://www.pymol.org.).

## Author Contributions

Conceived and designed the experiments: HK MT. Performed the experiments: MS HK KG KM AY MN. Analyzed the data: AR RT HI HT KK NO. Contributed reagents/materials/analysis tools: FT TS MK. Wrote the paper: HK MS MT.

## References


1. Griffin DE (2007) Measles viruses. In: Knipe DM, Howley PM, editors. Fields virology. 5th ed. Vol. 2. Philadelphia: Lippincott Williams & Wilkins. 1551–1585.
2. Griffin DE, Oldstone MBA (2009) Measles: Pathogenesis and control. Berlin: Springer-Verlag. 292 p.
3. Centers for Disease Control and Prevention (CDC) (2012) Progress in global measles control, 2000–2010. MMWR Morb Mortal Wkly Rep 61: 73–78.
4. World Health Organization (2006) Global distribution of measles and rubella genotypes-update. WER 81: 469–480.
5. Hashiguchi T, Kajikawa M, Maita N, Takeda M, Kuroki K, et al. (2007) Crystal structure of measles virus hemagglutinin provides insight into effective vaccines. Proc Natl Acad Sci U S A 104: 19535–19540.
6. Hashiguchi T, Ose T, Kubota M, Maita N, Kamishikiryo J, et al. (2011) Structure of the measles virus hemagglutinin bound to its cellular receptor SLAM. Nat Struct Mol Biol 18: 135–141.
7. Woelk CH, Holmes EC (2001) Variable immune-driven 415 natural selection in the attachment (G) glycoprotein of respiratory syncytial virus (RSV). J Mol Evol 52: 182–192.
8. Mizuta K, Saitoh M, Kobayashi M, Tsukagoshi H, Aoki Y, et al. (2011) Detailed genetic analysis of hemagglutinin-neuraminidase glycoprotein gene in human parainfluenza virus type 1 isolates from patients with acute respiratory infection between 2002 and 2009 in Yamagata prefecture, Japan. Virol J 8: 533.
9. Thorne JL, Kishino H, Painter IS (1998) Estimating the rate of evolution of the rate of molecular evolution. Mol Biol Evol 15: 1647–1657.
10. Lepage T, Bryant D, Philippe H, Lartillot N (2007) A general comparison of relaxed molecular clock models. Mol Biol Evol 24: 2669–2680.
11. Riddell MA, Rota JS, Rota PA (2005) Review of the temporal and geographical distribution of measles virus genotypes in the prevaccine and postvaccine eras. Virol J 2: 87.
12. World Health Organization (2010) Programmatic feasibility reports - per region and including comprehensive epidemiological data. WPRO: WPRO Feasibility Report. Available: http://www.who.int/immunization/sage/previous_november2010/en/index.html. Accessed: 2012 Feb 13.
13. Zhu Z, Cui A, Wang H, Zhang Y, Liu C, et al. (2012) Emergence and continuous evolution of genotype 1E Rubella viruses in China. J Clin Microbiol 50: 353–363.
14. Yoshida A, Kiyota N, Kobayashi M, Nishimura K, Tsutsui R, et al. (2012) Molecular epidemiology of attachment glycoprotein (G) gene in respiratory syncytial virus in children with acute respiratory infection in Japan in 2009/2010. J Med Microbiol. In press.
15. Webster RG, Bean WJ, Gorman OT, Chambers TM, Kawaoka Y (1992) Evolution and ecology of influenza A viruses. Microbiol Rev 56: 152–179.
16. Domingo E (2007) Virus evolution. In: Knipe DM, Howley PM, editors. Fields virology. 5th ed. Vol. 2. Philadelphia: Lippincott Williams & Wilkins. 389–421.
17. Loewe L (2008) Negative selection. Nature Education: 1.
18. Woelk CH, Jin L, Holmes EC, Brown DW (2001) Immune and artificial selection in the haemagglutinin (H) glycoprotein of measles virus. J Gen Virol 82: 2463–2474.
19. Corey EA, Iorio RM (2009) Measles virus attachment proteins with impaired ability to bind CD46 interact more efficiently with the homologous fusion protein. Virology 383: 1–5.
20. World Health Organization (2012) Measles virus nomenclature update: 2012. WER 87: 73–80.
21. Drummond AJ, Rambaut A (2007) BEAST: Bayesian evolutionary analysis by sampling trees. BMC Evol Biol 7: 214.
22. Pond SL, Frost SD (2005) Datamonkey: Rapid detection of selective pressure on individual sites of codon alignments. Bioinformatics 21: 2531–2533.
23. dos Reis M, Yang Z (2011) Approximate likelihood calculation on a phylogeny for Bayesian estimation of divergence times. Mol Biol Evol 28: 2161–2172.

Journal of Medical Virology 84:705–710 (2012)

# Phylogenetic Analysis of Rubella Viruses in Vietnam During 2009–2010

**Dinh Nguyen Tran,[1,2] Ngan Thi Kim Pham,[1] Thi Thuy Trinh Tran,[3] Pattara Khamrin,[4] Aksara Thongprachum,[1] Katsuhiro Komase,[5] Satoshi Hayakawa,[6] Masashi Mizuguchi,[1] and Hiroshi Ushijima[1,6]***

[1]*Department of Developmental Medical Sciences, School of International Health, Graduate School of Medicine, The University of Tokyo, Tokyo, Japan*
[2]*Department of Pediatrics, University of Medicine and Pharmacy at Ho Chi Minh City, Ho Chi Minh City, Vietnam*
[3]*An Binh Hospital, Ho Chi Minh City, Vietnam*
[4]*Department of Microbiology, Faculty of Medicine, Chiang Mai University, Chiang Mai, Thailand*
[5]*Department of Virology III, National Institute of Infectious Diseases, Tokyo, Japan*
[6]*Division of Microbiology, Department of Pathology and Microbiology, Nihon University, School of Medicine, Itabashi-ku, Tokyo, Japan*

Rubella virus (RV) usually causes a mild disease. However, infection during the first trimester of pregnancy often leads to severe birth defects known as congenital rubella syndrome (CRS). Although wild-type RVs exist and circulate worldwide, their genotypes remain unknown in many countries. The aim of this study was to identify the molecular characteristics of RVs found in Vietnam during the years 2009–2010 and to provide the first data concerning RV genotypes in this country. Throat swab samples were collected between 2009 and 2010 from four CRS cases and nine rubella infection cases visiting one Children's Hospital and one outpatient clinic in Ho Chi Minh City. The 739-nucleotide coding region of the RV E1 gene recommended by the World Health Organization was amplified by reverse transcriptase PCR, and the resulting DNA fragments were then sequenced. Sequences were assigned to genotypes by phylogenetic analysis with RV reference strains. RV RNA was detected in 11 clinical specimens. Phylogenetic analysis of the sequences showed that all 11 strains belonged to 2B genotype. Several variations in amino acids were found, among which five changes were involved in the B and T cell epitopes. These data indicate that viruses of genotype 2B were circulating in Vietnam. The increasing information about RV genotype in Vietnam should aid in the control of rubella infection and CRS in this country. ***J. Med. Virol. 84:705–710, 2012.*** © 2012 Wiley Periodicals, Inc.

**KEY WORDS:** genotype; molecular; characterization



## INTRODUCTION

Rubella infection is a mild disease that affects mainly children and young adults. It is characterized by a mild fever along with non-confluent maculopapular rash and lymphadenopathy [Reef et al., 2002; Banatvala and Brown, 2004]. However, infection during the first trimester of pregnancy can lead to abortions, miscarriages, stillbirths, and severe birth defects, known as congenital rubella syndrome (CRS) [Plotkin, 2001]. Although an effective vaccine is available, rubella is still an important public health concern [Cutts et al., 1997].

Rubella virus (RV) is the only member of the genus Rubivirus in the family *Togaviridae*. It has a spherical shape approximately 60–70 nm in diameter with a lipid envelope. The genome of RV is a single-stranded RNA of positive sense, which is 9,762 nucleotides (nts) in length. The genome has an unusually high proportion of guanosine and cytidine residues and contains two non-overlapping open reading frames (ORFs) [Dominguez et al., 1990]. The 5′ proximal ORF encodes non-structural proteins p150 and p90, which function in viral RNA synthesis. The 3′ proximal ORF

Grant sponsor: Japan Society for the Promotion of Science; Grant sponsor: Ministry of Health, Labor, and Welfare, Japan; Grant sponsor: Asian Development Bank.

Conflict of interest: none declared.

*Correspondence to: Hiroshi Ushijima, MD, PhD, Division of Microbiology, Department of Pathology and Microbiology, Nihon University, School of Medicine, 30-1 Oyaguchi-Kamicho, Itabashi-ku, Tokyo 173-8610, Japan.
E-mail: ushijima-hiroshi@jcom.home.ne.jp

Accepted 10 November 2011
DOI 10.1002/jmv.23199
Published online in Wiley Online Library (wileyonlinelibrary.com).

encodes three structural proteins, the capsid (C) and two glycoproteins, E1 and E2 [Frey, 1994]. These two glycoproteins heterodimerize to form the spike complexes that are embedded into the lipid envelope. The E1 glycoprotein plays an important role in binding to the host cell receptor and in fusing the viral envelope with the host cell membrane and includes an antigenic determinant that serves as a target for neutralizing antibodies [Hobman and Chantler, 2007]. Many genotypes of wild-type RVs exist and circulate worldwide. Based on the window of 739 nts within the E1 gene (nt 8731–9469) recommended by the WHO, nine recognized (1B, 1C, 1D, 1E, 1F, 1G, 2A, 2B, and 2C) and four provisional genotypes (1a, 1h, 1i, and 1j) of RVs have been defined [WHO, 2005; WHO, 2007]. Knowledge about the circulating RV genotypes in many countries is now increasingly available. However, the genotypes circulating in many others, including Vietnam, are still unknown.

In Vietnam, the rubella surveillance was integrated into the measles elimination system, but rubella vaccine is not included in the national immunization program. Rubella infection was found to be the most frequent cause of non-measles rash [WHO WPR, 2010]. In Vietnam, the incidence of rubella remains high in 2009, over 10 per million populations. Fifty-five percent of female rubella cases were reported among child-bearing-age women. No data about CRS in Vietnam are available [WHO WPR, 2010].

The aim of this study was to present the genotypes and molecular characteristics of wild-type RVs circulating in Vietnam during 2009–2010.

## MATERIALS AND METHODS

### Specimens

Throat swab samples were collected from three serologically confirmed infants with CRS and nine clinically suspected rubella infection patients from the Children's Hospital 2 and one outpatient clinic at Ho Chi Minh City in 2009 and 2010. The RV sequence from one CRS case reported previously was also included in this study [Tran et al., 2011]. Informed consent was obtained from all patients or their families. This study was approved by the ethics committees of the Children's Hospital 2.

### RNA Extraction and Reverse Transcription (RT)

RNA genome was extracted directly from clinical samples and RT was performed as previously described [Yan et al., 2003]. Briefly, RV RNA was heated to 95°C for 5 min and kept on ice before adding the reaction mixture and incubated at 55°C for 1 hr, followed by 95°C for 5 min and then rapidly cooled on ice.

### Polymerase Chain Reaction (PCR)

Two pairs of primers were chosen to cover the window of 739 nts within the E1 gene recommended by the WHO as previously described [Martínez-Torres et al., 2009]. The total volume 25 μl of the first-round PCR reaction mixture was consisted of 3 μl cDNA, 5 μl of 5× Taq DNA polymerase buffer (Promega, Madison, WI), 0.4 mM dNTPs, 0.5 μM each of the first-round primers GRUB739F1 (5′-CCCACCGACACCGTGATGA-3′) and GRUBR1 (5′-CCAGGTCTGCCGGGTCTC-3′), 1.25 U of (5U/μl) Taq DNA polymerase (Promega), DMSO 5% and distilled water. The PCR was performed at 94°C for 3 min, followed by 40 cycles of 95°C for 1 min, 56°C for 1 min, 72°C for 90 sec, and a final extension at 72°C for 7 min, and then held at 10°C. For the nested PCR, 1 μl of the first-round product was used as the template in the PCR mixture as described above except that the second round primers (GRUB739F2: 5′-GTGATGAGCGTGTTCGCCC-3′ and GRUB765: 5′-GCDGTGGTGTGTGTGCC-3′) concentration was increased to 1 μM each and the annealing temperature was 55°C. The PCR products were run on 1.5% agarose gel, and the bands were visualized by SYBR Safe (Invitrogen, Tokyo, Japan) staining under ultraviolet light. The expected band size was 875 bp.

### Nucleotide Sequencing and Phylogenetic Analysis

The products of nested PCR were purified using the MinElute PCR Purification Kit (Qiagen, Hilden, Germany) and then sequenced bi-directionally by the commercial company (Macrogen Japan Corp., Tokyo, Japan) using the inner primers. The nt sequences were analyzed and compared with the WHO recommended reference strains of all genotypes. The sequence data and the phylogenesis were analyzed using BioEdit [Hall, 1999] v.7.0.5. A parsimony analysis was also conducted using MEGA version 3.1. The method was performed using close-neighbor interchange with a random option and with 1,000 bootstrap repetitions. Phylogenetic analysis of RV genomes detected was carried out based on the window of 739 nts within the E1 gene.

The sequences of RVs detected in this study have been submitted to GenBank and assigned accession numbers HQ893749-HQ893758. One sequence reported in previous study was submitted to the DNA Data Bank of Japan and can be found under accession number AB546233 [Tran et al., 2011].

## RESULTS

### RV Detection and Sequence Analysis

Of the 12 samples screened in this study, 10 tested positive by RT-PCR. These consisted of three CRS cases and seven rubella infection cases. The RV strains found in this study were named according to the WHO systematic nomenclature [WHO, 2005]. The 739-nt sequence of the region encoding amino acid residues 159–404 within the E1 glycoprotein recommended by the WHO of the 11 Vietnamese strains

(one from previous report) was analyzed, in comparison with the vaccine strain RVi/USA/64 (RA27/3US64) and the WHO 2B reference strains. The strains in this study exhibited 98 variable positions in the nt sequence with respect to vaccine strain RA27/3 but only eight in the amino acid sequence (Fig. 1). Of the nt changes, 88/98 were found at the third base and only 8 at the first and 2 at the second base of the codon. Of the eight non-synonymous alterations, five changes appeared at position 1, and two occurred at position 2 of the codon. There were two codons having nt substitutions at the first and third position simultaneously. RV strain RVs/HoChiMinh.VNM/40.10 had one additional variable nt at position 8 on the first base of the codon, causing a change in amino acid T161A. Sequence RVs/HoChiMinh.VNM/46.10 had one additional variable nt at position 527 on the first base of the codon, which remained silent. Four amino acid mutations, which were present in all of the sequences (H210Y, A333V, T337A, L377V), together with T161A were located in the T- and B-cell epitopes described by Chaye et al. [1993].

The nt difference between the Vietnamese strains ranged from 0.3% to 5.3% (between RVs/HoChiMinh.VNM/13.10 and RVs/HoChiMinh.VNM/43.09). The mean divergence within all Vietnamese sequences was 2.2% and 3.8% relative to the WHO 2B reference strains. Of these 11 patients, 10 were residing in Ho Chi Minh City and one CRS case was in Binh Duong province, which is about 30 km from Ho Chi Minh City.

### Phylogenetic Analysis

The phylogenetic tree is shown in Figure 2. The Vietnamese strains grouped with the 2B reference sequences and clustered into two distinct lineages. The first lineage consisted of three strains with a nt difference ranging from 0.7% to 1.4%. The remaining eight strains composed the second lineage with the intra-group variation ranging from 0.3% to 1.5% and were most closely related to RVs that circulated in Brazil in the late 2010s. The average nt sequence divergence between these two lineages was 4.4%.

## DISCUSSION

Phylogenetic analysis of the nt sequence within the E1 gene was used to study the molecular epidemiology of RV in the south of Vietnam during 2009 and 2010. Rubella-containing vaccine has not been introduced into the national immunization program in Vietnam but it is available in the private sector. As a result, RV still continues to circulate due to low vaccination coverage. It was of interest to examine the viruses from the country with low or no vaccine coverage in order to understand the genetic characterization in such this setting. The strains in this study were collected from the small area of southern Vietnam,

| Aa position | 161 | 202 | 210 | 266 | 279 | 333 | 337 | 377 |
|---|---|---|---|---|---|---|---|---|
| L78917-RVi/USA/64-Vaccine | T | D | H | R | V | A | T | L |
| RVi/TELAVIV.ISR/68 | | | Y | | | | A | V |
| RVi/WA.USA/16.00 | | | Y | | | V | A | V |
| RVi/ANHUI.CHN/00 | | | Y | | I | V | A | V |
| RVs/HoChiMinh.VNM/43.09 | | | Y | | | V | A | V |
| RVs/BinhDuong.VNM/44.09 | | | Y | | | V | A | V |
| RVs/HoChiMinh.VNM/24.10 | | | Y | | | V | A | V |
| RVs/HoChiMinh.VNM/12.10 | | | Y | | | V | A | V |
| RVs/HoChiMinh.VNM/13.10 | | | Y | | I | V | A | V |
| RVs/HoChiMinh.VNM/14.10 | | | Y | | | V | A | V |
| RVs/HoChiMinh.VNM/40.10 | A | | Y | | | V | A | V |
| RVs/HoChiMinh.VNM/41.10 | | N | Y | | | V | A | V |
| RVs/HoChiMinh.VNM/43.10 | | | Y | | | V | A | V |
| RVs/HoChiMinh.VNM/44.10 | | | Y | P | | V | A | V |
| RVs/HoChiMinh.VNM/46.10 | | | Y | | | V | A | V |

Fig. 1. Amino acid sequence alignment of the 739-nt window within the E1 gene (nt 8731–9469, aa 159–404) as recommended by the WHO of 11 Vietnamese strains, the vaccine strain RVi/USA/64 and the WHO 2B reference strains.

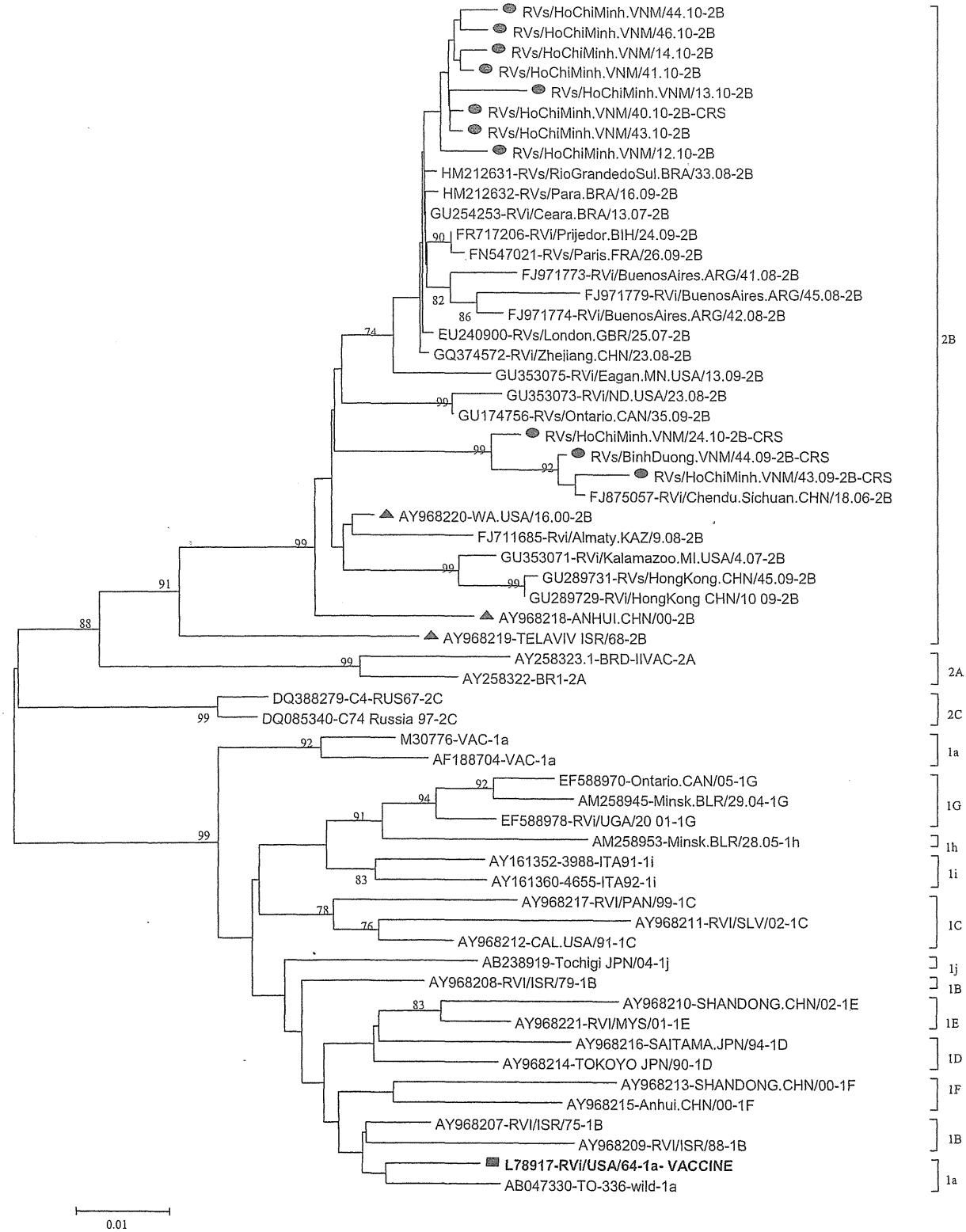


Fig. 2. Phylogenetic tree was constructed from the studied strains and the reference strains recommended by WHO and sequences obtained from GenBank using the window of 739 nts within the E1 gene (nt 8731–9469) with MEGA 3.1 software. Bootstrap values of >70% are shown at the branch nodes. The RV strains in this study are marked with solid round. WHO 2B reference strains are indicated by solid triangle, and the vaccine strain is indicated by solid square.

providing the genetic baseline information about the circulating genotypes. These baseline data should be useful in efforts to control rubella infection and CRS.

Phylogenetic analysis of the 11 sequences obtained during this study showed that genotype 2B was circulating in South Vietnam. Interestingly, these 2B sequences segregated into two separate lineages. The viruses that formed the first lineage shared 98–99% nt similarity by BLAST search to the genotype 2B strain RVi/Chendu.Sichuan.CHN/18.06/1[2B] isolated in Sichuan, China in 2006 (GenBank FJ875057.1). This strain was thought to have origin in Vietnam and was imported into China [Zhu et al., 2010]. Meanwhile, the viruses of second lineage showed the highest similarity to those that were circulating in Brazil during 2007–2009. However, the relation of this lineage to the circulating strains in Brazil cannot be determined. Genotype 2B viruses were previously known to circulate in China, India, South Korea, and South Africa [WHO, 2005; WHO, 2006; Caidi et al., 2008; Rajasundari et al., 2008] before being introduced into some countries in Europe [Jin and Thomas, 2007; Novo et al., 2009; D'Agaro et al., 2010; Vauloup-Fellous et al., 2010] and South America [Valinotto et al., 2009]. The variation observed in this study reflected the molecular characteristics of RVs in population with low vaccine coverage. As a result of multiple epidemics and importations, there might be many lineages within a genotype or many genotypes co-circulating. To establish the complete genetic baseline for RV Vietnamese strains, it is obvious that additional samples from other locations in the coming years need to be collected and analyzed.

Genetic divergences between the 11 strains in this study were not clearly geographically and chronologically related. The most divergence was 5.3% between case RVs/HoChiMinh.VNM/43.09 and case RVs/HoChiMinh.VNM/13.10. Both cases were from Ho Chi Minh City. On the other hand, the high difference (9.9–11.1%) was seen between these strains and the vaccine strain RA27/3, which is currently used in the private sector. This may be explained by the fact that the vaccine strain belongs to genotype 1a, another clade. Majority (90/98) of the nt position variations relative to the vaccine strain RA27/3 among the eleven Vietnamese sequences did not lead to amino acid substitutions, which is consistent with the findings of other reports [Bosma et al., 1996; Hübschen et al., 2007]. This confirms that RV is highly conserved at the amino acid level. Several mutations were involved in the immuno-reactive regions in the E1 glycoprotein, which contains the antigenic sites and has an important role in the antigenicity of RV [Terry et al., 1988; Chaye et al., 1992; Mitchell et al., 1992; Chaye et al., 1993; Ou et al., 1993]. Further investigation is required to better understand these mutations.

In conclusion, this is the first molecular epidemiological characterization of RVs that is endemic in Vietnam, in the setting of low vaccine coverage. Despite the data limitation, this study contributes to understanding the origin of RVs circulating in Vietnam and providing information to the worldwide genetic documentation of RV distributions. Molecular epidemiology has been shown to be valuable for the control and elimination of rubella infection and CRS. However, further study is necessary to establish the complete genetic baseline for this country.

## ACKNOWLEDGMENTS

We thank Dr. Nguyen Tran Quynh Nhu and Ms. Pham Thi Ngoc Hue, Cardiovascular Department, Children's Hospital 2, Ho Chi Minh City for their help in patient counseling and sample collection.

## REFERENCES

Banatvala JE, Brown DWG. 2004. Rubella. Lancet 363:1127–1137.

Bosma TJ, Best JM, Corbett KM, Banatvala JE, Starkey WG. 1996. Nucleotide sequence analysis of a major antigenic domain of the E1 glycoprotein of 22 rubella virus isolates. J Gen Virol 77:2523–2530.

Caidi H, Abernathy ES, Benjouad A, Smit S, Bwogi J, Nanyunja M, El Aouad R, Icenogle J. 2008. Phylogenetic analysis of rubella viruses found in Morocco, Uganda, Cote d'Ivoire and South Africa from 2001 to 2007. J Clin Virol 42:86–90.

Chaye H, Chong P, Tripet B, Brush B, Gillam S. 1992. Localization of the virus neutralizing and hemagglutinin epitopes of E1 glycoprotein of rubella virus. Virology 189:483–492.

Chaye H, Ou D, Chong P, Gillam S. 1993. Human T- and B-cell epitopes of E1 glycoprotein of rubella virus. J Clin Immunol 13: 93–100.

Cutts FT, Robertson SE, Diaz-Ortega JL, Samuel R. 1997. Control of rubella and congenital rubella syndrome (CRS) in developing countries, part 1: Burden of disease from CRS. Bull WHO 75: 55–68.

D'Agaro P, Dal Molin G, Zamparo E, Rossi T, Micuzzo M, Busetti M, Santon D, Campello C. 2010. Epidemiological and molecular assessment of a rubella outbreak in North-Eastern Italy. J Med Virol 82:1976–1982.

Dominguez G, Wang CY, Frey TK. 1990. Sequence of the genome RNA of rubella virus: Evidence for genetic rearrangement during togavirus evolution. Virology 177:225–238.

Frey TK. 1994. Molecular biology of rubella virus. Adv Virus Res 44: 69–160.

Hall TA. 1999. BioEdit: A user-friendly biological sequence alignment editor and analysis program for Windows 95/98/NT. Nucl Acids Symp Ser 41:95–98.

Hobman T, Chantler J. 2007. Rubella virus. In: Knipe DM, Howley PM, editors. Fields virology. 5th edition. Philadelphia, PA: Lippincott, Williams, and Wilkins, pp 1069–1100.

Hübschen JM, Yermalovich M, Semeiko G, Samoilovich E, Blatun E, De Landtsheer S, Muller CP. 2007. Co-circulation of multiple rubella virus strains in Belarus forming novel genetic groups within clade 1. J Gen Virol 88:1960–1966.

Jin L, Thomas B. 2007. Application of molecular and serological assays to case based investigations of rubella and congenital rubella syndrome. J Med Virol 79:1017–1024.

Martínez-Torres AO, Mosquera MM, Sanz JC, Ramos B, Echevarría JE. 2009. Phylogenetic analysis of rubella virus strains from an outbreak in Madrid, Spain, from 2004 to 2005. J Clin Microbiol 47:158–163.

Mitchell LA, Zhang T, Ho M, Décarie D, Tingle AJ, Zrein M, Lacroix M. 1992. Characterization of rubella virus-specific antibody responses by using a new synthetic peptide-based enzyme-linked immunosorbent assay. J Clin Microbiol 30:1841–1847.

Novo A, Huebschen JM, Muller CP, Tesanovic M, Bojanic J. 2009. Ongoing rubella outbreak in Bosnia and Herzegovina, March–July 2009—Preliminary report. Euro Surveill 14:pii-19343.

Ou D, Chong P, Tingle AJ, Gillam S. 1993. Mapping T-cell epitopes of rubella virus structural proteins E1, E2, and C recognized by T-cell lines and clones derived from infected and immunized populations. J Med Virol 40:175–183.